Nanoscale

ROYAL SOCIETY OF CHEMISTRY

MINIREVIEW

View Article Online
View Journal | View Issue

Check for updates

Cite this: *Nanoscale*, 2025, **17**, 10557

Recent progress of noble metal-based nanozymes: structural engineering and biomedical applications

Xiao Wang,† Chenhao Shu,† Gang Wang, Peng Han, Long Zheng, Lei Xu and Ye Chen *

Received 31st December 2024,
Accepted 18th March 2025

DOI: 10.1039/d4nr05514d

rsc.li/nanoscale

Due to their tunable catalytic activity, high chemical stability, and favorable electronic structure, noble metal-based nanozymes that can mimic important biocatalytic processes have attracted great attention. Rational structural design of noble metal-based nanozymes can endow them with excellent enzyme-like activities, enhanced sensitivity and stability, as well as unique physicochemical functionalities towards various biomedical applications such as sensing, diagnostics, and disease treatment. This review summarizes the recent progress in structural engineering of noble metal-based nanozymes and emphasizes the relationship between key structural factors of nanozymes and their enzyme-like properties in various enzyme-mimicking reactions. The diverse applications of noble metal-based nanozymes in biosensors, antibiosis, and disease treatment are further introduced. Finally, current challenges and future research directions in noble metal-based nanozymes are discussed. This review could offer scientific guidance to design and fabricate advanced nanozymes with enhanced functionality and performance towards clinical, environmental and biomedical applications.

1. Introduction

Natural enzymes are efficient catalysts for organisms and play key roles in various metabolisms, but their shortcomings such as susceptibility, complex preparation, and high price limit their practical applications in industrial, medical, and biological fields.[1] To overcome these disadvantages, researchers have devoted themselves to the exploration of artificial enzyme mimics.[2] Traditionally, various proteins and organic molecules have been explored as stable and low-cost alternatives to natural enzymes, but they still suffer from unsatisfactory performances compared with natural enzymes.[3] In recent years, nanozymes made of nanomaterials have received great interest owing to their tunable catalytic activities in mimicking the enzyme-like substrate-to-product conversion.[4] Notably, nanozymes can integrate their excellent catalytic activities with other unique physicochemical properties (*e.g.*, magnetic, optical, electrical properties) of nanomaterials, which often endows them with multiple functionalities.[5] Among the various kinds of nanozymes developed to date, noble metals such as gold (Au),[6–8] silver (Ag),[9,10] platinum (Pt),[11–13] palladium (Pd),[14–16] iridium (Ir),[17,18] ruthenium (Ru),[19,20] and rhodium (Rh)[12,21] are recognized as promising candidates due to their unique features such as excellent intrinsic catalytic activities,[22] high chemical stability, and outstanding optical and photothermal conversion properties, as well as remarkable local surface plasmon resonance (LSPR) effect. To date, noble metal based-nanozymes have been reported effective in mimicking a variety of enzyme-like processes, like those of peroxidase (POD),[23,24] catalase (CAT),[25–27] oxidase (OxD),[28,29] and superoxide dismutase (SOD).[30,31] More importantly, noble metal-based nanomaterials often possess unique plasmonic,[32,33] electrical,[18] magnetic,[34] and thermal[35] properties that can be smartly integrated into multifunctional nanozymes by structural engineering. For example, plasmonic noble metal nanomaterials (Au, Ag, and Pd), whose optical spectra closely rely on their size, shape, and compositions, are widely used in photothermal therapy (PTT) and photodynamic therapy (PDT).[35–38] Meanwhile, owing to the X-ray attenuation capability of noble metals (Au, Pt, Ir, *etc.*), noble metals are also ideal imaging contrast agents for X-ray computed tomography (CT) and photoacoustic imaging (PAI).[39–41] Therefore, noble metal-based nanozymes have great potential to integrate the enzyme-like function with imaging, biosensing, and treatment *via* leveraging the synergistic effects of their unique optical and catalytic properties. As a result, noble metal-based nanozymes have proved very promising in a variety of biomedical applications such as biosensors,[42,43] antioxidation,[44,45] cancer therapy,[46,47] immunoassays,[28] *etc.*

The integrated enzyme-like behaviors of noble metal-based nanozymes were found to be closely related to their size,[48]

Department of Chemistry, The Chinese University of Hong Kong, Shatin, New Territories, Hong Kong SAR, China. E-mail: yechen@cuhk.edu.hk
†These authors contributed equally to this review.

surface structure (*e.g.*, facet, phase, and defect),[49,50] ligand,[51] and composition.[52,53] For instance, reducing the size of nanozymes is an efficient strategy to optimize the catalytic efficiency with an enlarged specific surface area[15,48] and optimized biocompatibility.[54] Surface engineering is another important aspect to functionalize nanozymes by modulating their exposed facets,[49] crystal phase,[23,55] type of ligand,[51,56] and defects,[35,57] which would distinctly affect the interaction between the nanozyme surface and catalytic intermediates. With rational design and precise synthesis, the atom utilization efficiency, selectivity, activity, and multi-functionality of surface-engineered noble metal nanozymes could be greatly optimized.[34,52,53] Moreover, constructing noble metal-based nanoheterostructures can further regulate the enzymatic activity and expand their potential bioapplications. By introducing a second metal or nonmetal components, nanoheterostructures can achieve various effects such as theragnostics, targeted therapy, and cascade biocatalysis.

Altogether, structural engineering is crucial for developing promising noble metal-based nanozymes with tailorable catalytic performances and multi-functionalities as well as expanded potential applications. In this review, we present an overview of the latest progress in the structural design, enzymatic behaviors, and biomedical applications of noble metal-based nanozymes (Fig. 1). First, the structural factors of noble metal nanozymes that affect enzymatic activity, selectivity, and stability are introduced. The additional functions brought by these structural factors are also discussed. Representative strategies to construct various noble metal-based heterostructures, including single-atom nanozymes (SAzymes), towards further enhanced enzyme-like properties and multiple functionalities are presented. Subsequently, the enzyme-like catalytic behaviors of noble metal-based nanozymes are summarized. Then, the applications of noble metal-based nanozymes in biosensors, antibiosis, and disease treatment are demonstrated. Finally, some major challenges and prospective opportunities in this research field are discussed.

2. Structural engineering for noble metal-based nanozymes

Understanding the roles played by structural factors of noble metal-based nanomaterials plays a fundamental role in revealing their structure–property–performance relationship. Great advances have been achieved in the past few years in understanding the effects of several structural factors, including size, facet, strain, crystallinity, alloying, and ligands, of noble metal nanozymes on enhancing their activity, selectivity, and multi-functionalities. In addition, heterostructures synthesized by incorporating a second component into noble metals have also emerged as promising nanozymes. Noble metal-based nanozyme heterostructures can induce geometric, compositional, and electronic effects, thereby optimizing the activity and bringing more intriguing possibilities. In section 2, we systematically summarize these strategies to realize structural engineering of noble metal-based nanozymes.

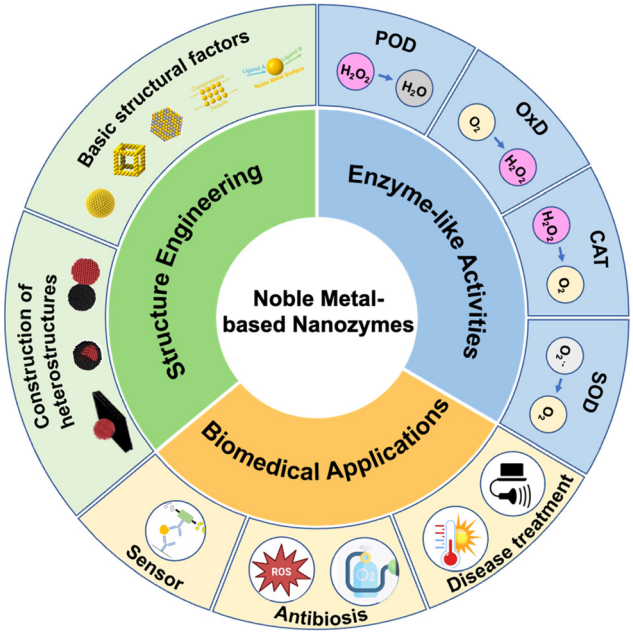

Fig. 1 Schematic overview of the structural engineering, enzyme-like activities, and biomedical applications of noble metal-based nanozymes.

2.1 Structural factors in noble metal nanozymes

2.1.1 Size. Size control of nanomaterials plays a vital role in the conventional catalytic process, which is often achieved by simply varying the reaction duration or the concentration of starting precursor.[58,59] In general, a smaller size of nanozymes shows higher catalytic efficiency due to larger specific surface area and higher density of active surface atoms. Xia *et al.* demonstrated the POD-like activity of Pd–Ir core–shell nanoparticles (NPs) with four different size (3.3, 5.9, 9.8, and 13.0 nm).[15] With size decreased to 3.3 nm, the NPs possess larger specific surface with greater diffusivities and reduced steric effect, which could promote the antibody–antigen interaction when applied in enzyme-linked immunosorbent assay (ELISA). As a result, the limit of detection (LOD) values of those NPs were lowered from 9.3 to 8.2, 4.6, and 3.7 pg mL^{-1} when the size was reduced from 13.0 to 9.8, 5.9, and 3.3 nm, respectively. Additionally, size has also been reported to regulate the surface oxidation state of noble metals.[48] A size-controlled synthesis method was adopted to prepare three types of Ru NPs (2 nm: sRuNP; 3.9 nm: mRuNP; 5.9 nm: lRuNP) (Fig. 2a–c). As shown in Fig. 2d, the ratio of oxidized Ru on the surface of Ru NPs increased linearly with the surface area, and the smallest sRuNP reached a maximal ratio of oxidized Ru of over 90%. It was found that sRuNPs exhibited higher antioxidant activity as CAT-like mimics when compared with their larger-size counterparts, which may be related to the more oxidized surface Ru atoms (Fig. 2e and f). Notably, based on their antioxidant enzyme-like activities and ultrasmall size, sRuNPs

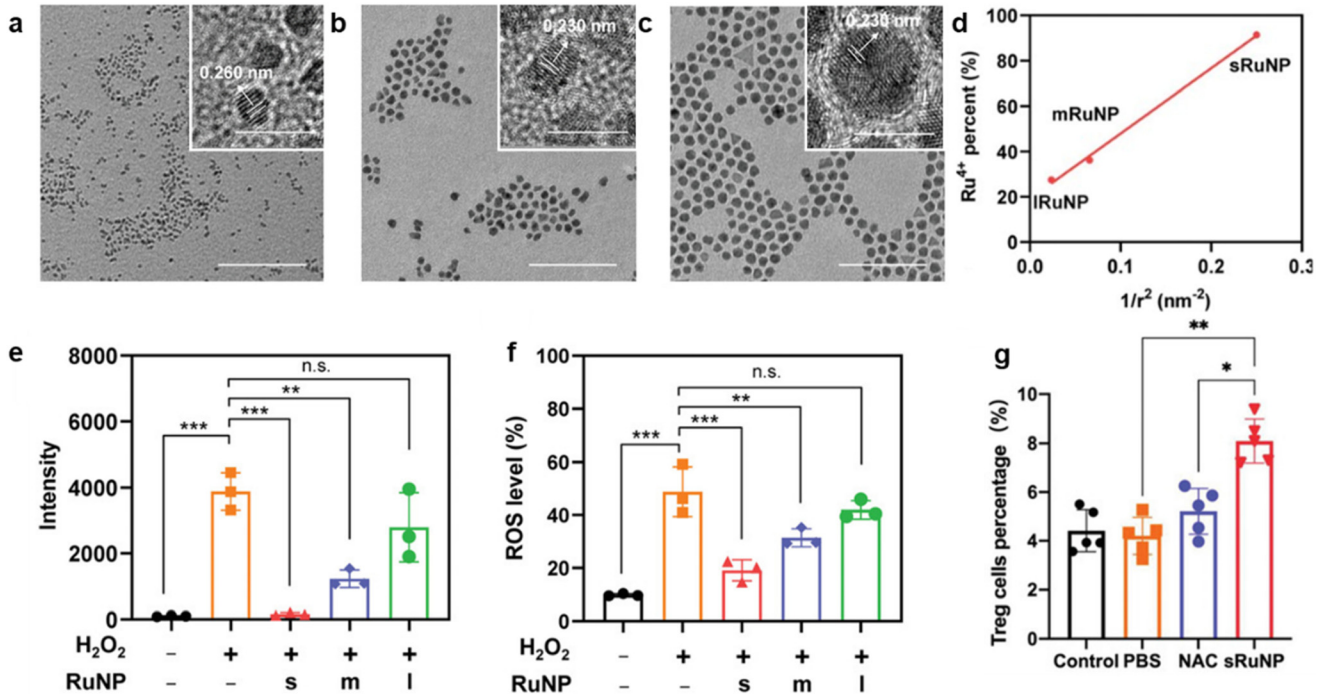

Fig. 2 Transmission electron microscopy (TEM) (scale bar: 50 nm) and high-resolution TEM (HRTEM) images (scale bar in insets: 5 nm) of (a) 2 nm Ru NPs (sRuNP), (b) 3.9 nm (mRuNP), and (c) 5.9 nm Ru NPs (lRuNP). (d) The correlation fitting curve between the ratio of Ru^{4+} (oxidized Ru) and the surface to volume ratio of different Ru NPs. Catalase-like (CAT-like) catalytic behaviors of different-sized Ru NPs in terms of (e) degree of intracellular oxidative stress of liver cells (L02) after being treated with H_2O_2 (200 μm) for 4 h, and (f) flow cytometry analysis of reactive oxygen species (ROS) in the cells. (g) The percentage of Treg cells recorded in liver tissues of mice with acetaminophen-induced liver injury after different treatments, showing advantageous internalization of sRuNP by Treg cells *in vivo* therapy (control: without any treatment. PBS: treated with phosphate buffered saline solution. NAC: treated with *N*-acetylcysteine solution. sRuNP: treated with sRuNP). Reproduced with permission from ref. 48. Copyright 2022, Wiley-VCH.

can not only facilitate internalization by Treg cells and persist for a long time, but also sustainably ameliorate oxidative stress, thus alleviating severe liver injury, with a significantly long therapeutic time window for *in vivo* therapy (Fig. 2g). Therefore, size effect not only modifies the catalytic activity of nanozymes by adjusting the specific surface area and modifying the electronic structure of surface atoms, but also affects their biocompatibility. For these reasons, fine size control is essential for biomedical applications of noble metal nanozymes.

2.1.2 Morphology and facet. It is generally accepted that the activity of a catalyst is determined by the morphology in terms of both specific surface area and active sites.[60,61] To improve metal utilization efficiency and increase the number of active sites, elegant design of the morphology of nanozymes has emerged as a research hotspot. To date, nanozymes with numerous morphologies have been reported. Complex 3D morphologies, such as nanodendrites,[62,63] nanoframes,[64–66] nanoflowers,[67,68] and hollow structures[69] possess a high density of surface active sites and unique optical features that can be employed for nanozyme applications. For example, Zheng *et al.* obtained hollow nanocages of $PdPt_3$ and $PdIr_3$ by etching core/shell Pd/Pt and Pd/Ir nanocubes. The unique hollow structure had a porous surface surrounded by an ultrathin frame, which greatly improved their catalytic efficiency for uricase degradation and H_2O_2 elimination under physiological conditions. The cubic hollow $PdPt_3$ and $PdIr_3$ nanocages showed high activity toward self-cascade uricase/POD-like catalytic reactions.[70] In another work, Pt hollow nanodendrites were synthesized by selective removal of Pd cores in Pd@Pt core–frame nanodendrites, which showed higher POD-like activity than Pd nanocubes and Pd@Pt core–frame nanodendrites.[62] The authors explained that both nanodendrite shells with large specific area and hollow structures with porous surfaces significantly enhanced the POD-like properties of Pt hollow nanodendrites. Moreover, the morphology-dependent optical properties of plasmonic noble metals can also be synergistically integrated into nanozymes. For example, Jia *et al.* synthesized flower-like AgPd blackbody nanozymes, with intense LSPR absorption in a broad spectral range from 400 to 1300 nm.[67] As a result, the hyperbranched AgPd blackbody nanozymes delivered prominent photothermal efficiency (η = 45.1%) *in vitro* and realized a localized photothermal response *in vivo* through tissue-penetrating near-infrared (NIR)-II light. Furthermore, the photothermal effect could significantly elevate the POD-like activity as well as the CAT-like activity to relieve tumor hypoxia.

Meanwhile, researchers found that the poorly defined shapes of nanomaterials make it difficult to establish a clear structure–property–performance relationship. Thanks to continuous research efforts, colloidal synthesis has been success-

ful in producing noble metal nanocrystals bearing well-defined shapes, leading to the identification of specific facets. In the past decade, both experimental and computational studies have been established to prove that enzyme-like performances are highly sensitive to the exposed facets. For instance, concave Au/Cu nanorods (NRs) with high-index (200) facets were synthesized *via* etching Au NRs with Cu^{2+} ions.[71] The catalytic activity of Au/Cu NRs was confirmed by the oxidation of colorless 3,3′,5,5′-tetramethylbenzidine (TMB) to blue oxidized TMB by H_2O_2. With the presence of more tips and high-index facets, the K_{cat}/K_m (K_{cat}, catalytic constant; K_m, Michaelis constant) value of Au/Cu NRs was 781.3 μM^{-1} min^{-1}, which is 4.5 times higher than that of Au NRs (172.8 μM^{-1} min^{-1}). Furthermore, the facet-dependent OxD-like property of Pd nanocrystals was studied by Zhou's group.[49,72] The (100)-faceted Pd cubes nanozymes exhibited higher activities for H_2O_2 generation than (111)-faceted Pd octahedra (Fig. 3a–g),[72] while the Pd concave nanocubes with high-index (730) facets were reported to have better OxD-like activity than (111) facets due to the undulating surface composed of highly unsaturated Pd atoms (Fig. 3h–k).[49] Recently, holey Pd nanosheets with highly active Pd(100) facets were prepared by anisotropic oxidative etching, which showed enhanced CAT-like activity compared with the intact Pd nanosheets only exposing (111) facets. The high efficiency for the decomposition of H_2O_2 to O_2 and the ability to generate singlet oxygen ($^1O_2$) from O_2 make holey Pd nanosheets great nanozyme candidates against hypoxic tumors.[73] In addition to these experimental efforts, theoretical calculations also provide evidence for facet-dependent activities of noble metal nanozymes. The facet-dependent OxD-like properties of Au, Ag, Pd and Pt were predicted *via* the density functional theory (DFT) method,[74] in which the dissociation of O_2 on various metal surfaces was evaluated to predict their OxD-like activities. Ag(111) and Au(111) were found to possess high activation and reaction energies, therefore were both thermodynamically and kinetically unfavored for dissociative adsorption of O_2. Thus, the predicted sequence of OxD activities of the (111) facet is Pd > Pt ≫ Au and Ag. Facets with higher energies like (211) of Au were also studied. Compared with the Au(111) facet, the high-index (211) facet had a better performance due to the strong dissociative adsorption of O_2.

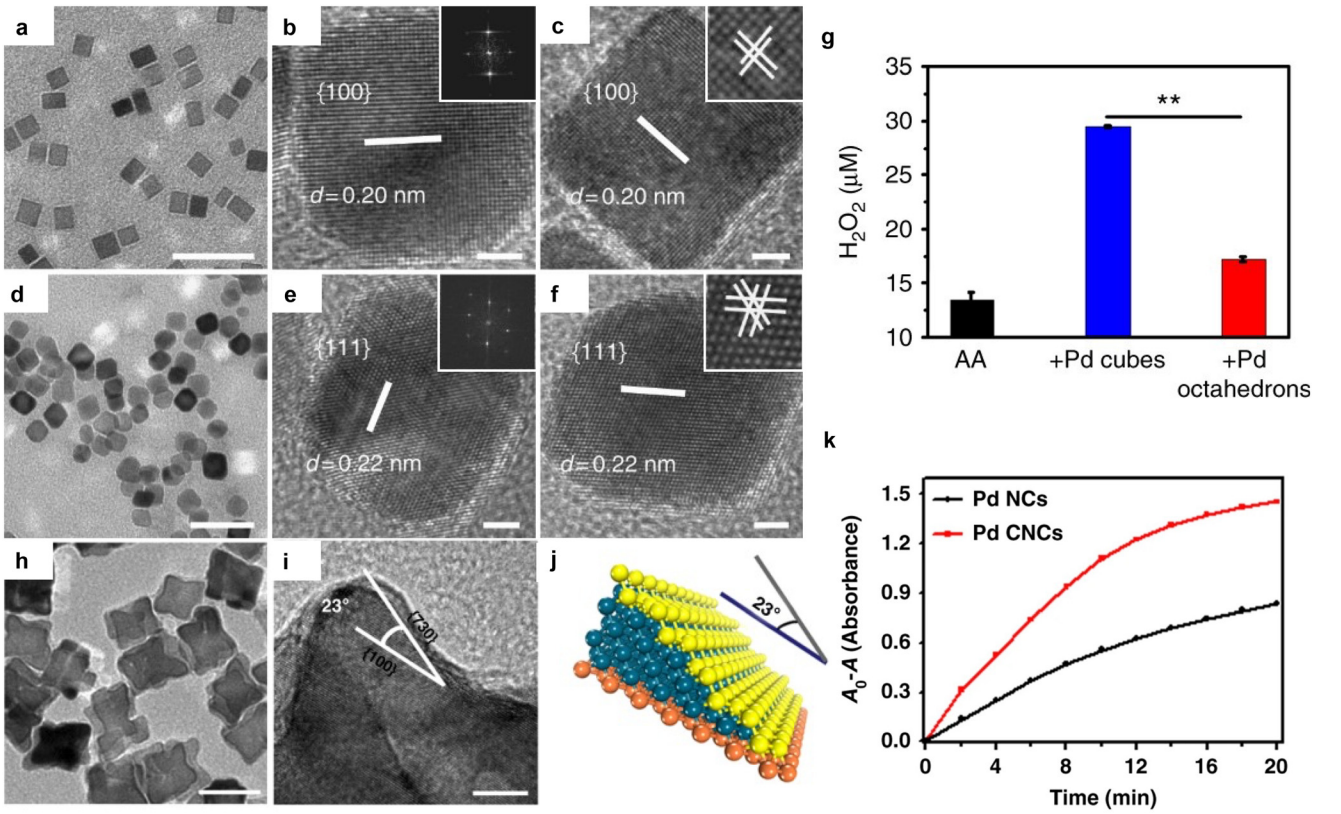

Fig. 3 (a) TEM image (scale bar: 20 nm), (b and c) HRTEM images (scale bar: 2 nm), and corresponding fast Fourier transformation (FFT) pattern (inset) of (100)-faceted Pd cubes. (d) TEM image (scale bar: 20 nm), (e and f) HRTEM images (scale bar: 2 nm), and corresponding FFT pattern (inset) of (111)-faceted Pd octahedra. (g) Comparison of concentrations of H_2O_2 generated using different Pd nanozymes, showing a facet-dependent oxidase-like (OxD-like) activity. AA (ascorbic acid), as a physiologically relevant antioxidant, was used as substrate to assess the OxD-like activities of Pd nanocrystals. Reproduced with permission from ref. 72. Copyright 2018, Springer Nature Limited. (h) TEM image of (730)-faceted Pd concave nanocubes (Pd CNCs) (scale bar: 50 nm), (i) HRTEM image of Pd CNCs (scale bar: 5 nm), and (j) model of the atomic arrangement on the (730) surface of Pd CNCs. (k) Comparison of absorbance changes of substrate using Pd nanocubes (NCs) or Pd CNCs, showing a facet-dependent OxD-like activity. Reproduced with permission from ref. 49. Copyright 2018, Springer Nature Limited.

2.1.3 Strain. Reports suggest that nanomaterials can withstand up to ~10% lattice strain.[75,76] Specifically, expanded lattice distance reflects tensile strain while shortened lattice distance gives compressive strain.[77] Lattice strain may be caused by size/shape variation,[78] doping,[79] lattice mismatch,[80] and structural defects,[81] and has been verified to modify the surface properties and further promote the catalytic performance[57,82,83] of noble metal nanozymes. For example, Pd octahedra with unstrained (111) facets and Pd icosahedra with strained (111) facets were synthesized (Fig. 4a and b). The tensile strain is indicated by the right-shifted XRD peaks, while the compressive strain is represented by the small hump (Fig. 4d).[82] The strained Pd icosahedra were found to display 2-fold higher POD-like catalytic efficiency than the unstrained Pd octahedra. The authors explained that the expansive strain in Pd icosahedra may be beneficial for key intermediate generation, thus improving the enzymatic performance (Fig. 4c).[82] Furthermore, Li *et al.* found that lattice tensile strain and surface reconstruction could be induced on Pd nanosheets stored in ethanol at room temperature.[57] HRTEM was employed to verify the lattice spacing and a lattice spacing expansion of around 6.9% in Pd nanosheets was observed (Fig. 4e–g). The strained Pd(111) nanosheets exhibited enhanced CAT-like activity for O_2 production from H_2O_2 (Fig. 4h). Additionally, some core–shell structures with strain effect caused by lattice mismatch were also reported to enhance the enzyme-like activities. Xia *et al.* successfully synthesized a Pd–Ir core–shell nanocube and the lattice mismatch between Ir overlayers and Pd cores induced the lattice strain.[83] The K_{cat} values of the four different $PdIr_x$ (x = 0.036, 0.046, 0.062, and 0.116) samples toward both TMB and H_2O_2 showed a volcano-shaped dependence on the Ir content, with the maximum point corresponding to $PdIr_{0.062}$. The increased activity of $PdIr_x$ was related to the Ir shell thickness. The

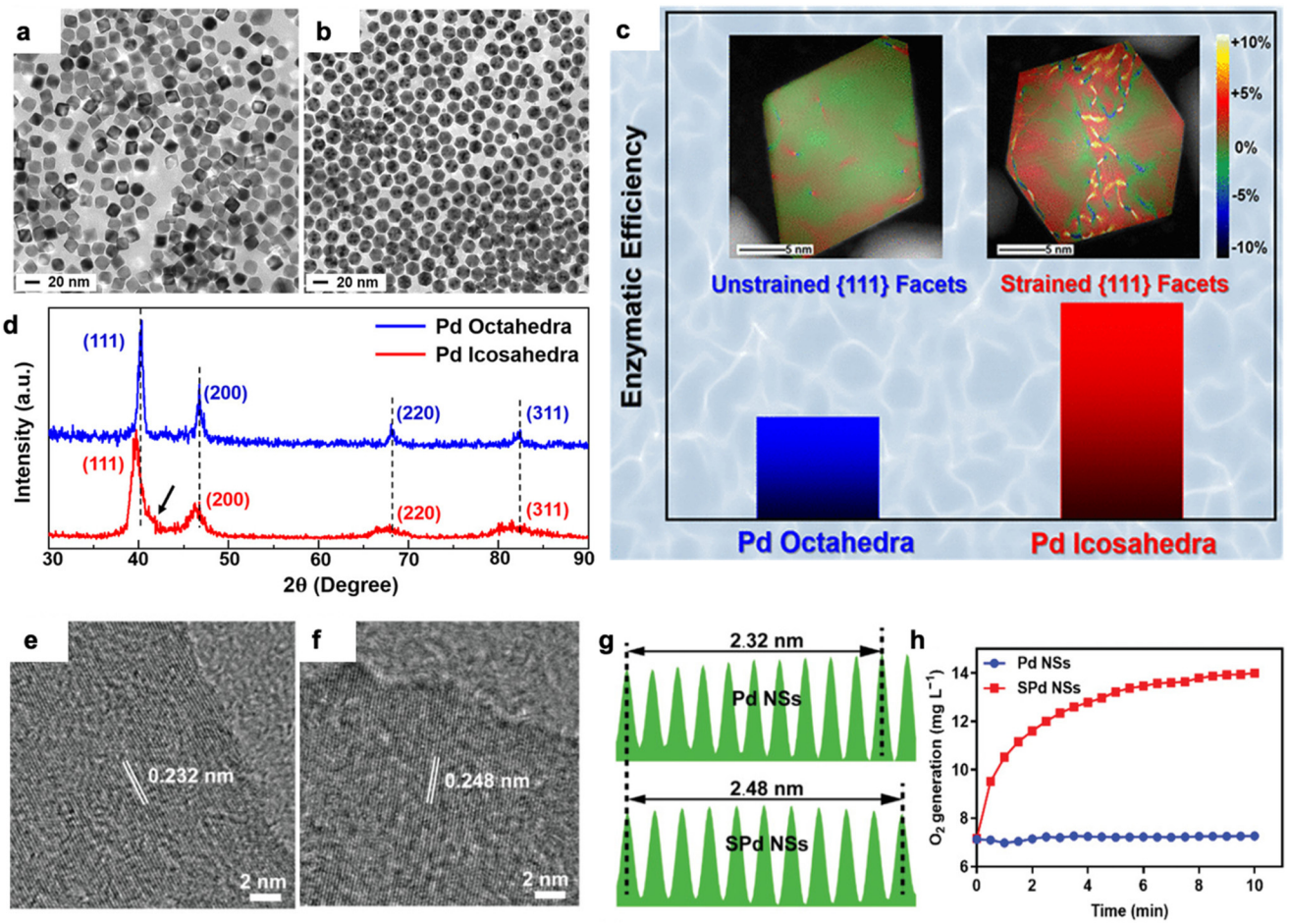

Fig. 4 TEM images of (a) Pd octahedra and (b) Pd icosahedra nanozymes. (c) A histogram comparing the peroxidase-like (POD-like) efficiency and surface strain mappings (inset) of Pd octahedron and icosahedron. (d) X-ray diffraction (XRD) patterns of Pd octahedra and icosahedra. The dashed line compares the peak shift of (111) between the Pd icosahedron and octahedron, indicating a possible tensile stress in the icosahedron. The small hump indicated by the black arrow was believed to reflect the presence of compressive stress in the icosahedron. Reproduced with permission from ref. 82. Copyright 2019, American Chemical Society. HRTEM images of (e) Pd nanosheets (Pd NSs) and (f) strained Pd NSs (SPd NSs), as well as (g) their lattice spacing measurements. (h) Comparison of CAT-like catalytic behaviors of Pd NSs and SPd NSs. The O_2 generation upon the addition of 10 mM H_2O_2 and 5 μg mL^{-1} nanozymes in a neutral buffer shows a clear difference. Reproduced with permission from ref. 57. Copyright 2022, Wiley-VCH.

tensile strain of the Ir shell and its stronger adsorption ability for oxygen-containing species helped to increase the reactivity, but the strain effect would be shielded when the Ir shell was too thick. In addition, the presence of an amorphous-crystalline hetero-phase can also induce the strain effect. For example, a tensile strain-mediated amorphous–crystalline RhRu bimetallene nanozyme was synthesized and found to possess CAT-like and POD-like activities.[35] The strain value of RhRu bimetallic crystalline–amorphous heterophase boundaries is around 2%, which is beneficial for modulating the adsorption capacities and energies of substrates, intermediates, and products during the reactions.

2.1.4 Crystallinity. Degree of crystallinity in noble metal nanomaterials refers to the extent of long-range atomic ordering. Crystallinity regulation, as a part of crystal phase regulation,[84,85] has emerged as an effective method to tune their physicochemical properties, particularly in a variety of catalytic applications.[86]

While the crystalline phase is mostly obtained in noble metal nanomaterials, the amorphous phase with a highly disordered atom arrangement, which is thermodynamically unfavorable, has also been obtained. Crystallinity control has been realized by annealing,[87,88] tuning reaction temperature,[89] choosing appropriate reducing agents,[90] and doping.[91–94] For example, ultrathin Ru nanosheets with different crystallinity were synthesized by using different potassium salts during annealing treatment, resulting in amorphous (Fig. 5a–c) and crystalline (Fig. 5e–g) Ru nanosheets of similar thickness.[88] The randomly distributed atoms with blurred diffraction ring verified the successful synthesis of amorphous Ru nanosheets (Fig. 5b), while crystalline Ru nanosheets showed a clear lattice with multiple diffraction rings (Fig. 5f). The degree of amorphousness of Ru nanosheets exhibited a positive relationship with the POD-like activity (Fig. 5d). The author explained that the enhanced POD-like activity and selectivity of amorphous Ru nanosheets were related to the increased H_2O_2 affinity caused by the amorphous surface. Additionally, amorphous noble metal compounds including $IrTe_2$ [55] and $RuTe_2$ [95] also have been reported to exhibit enhanced enzymatic performance compared with their crystalline counterparts. Briefly, the amorphous $RuTe_2$ NRs POD-like nanozymes showed a 3.77-fold higher K_{cat} and better substrate affinity than their crystalline structure counterparts.[95] Defect-rich glassy $IrTe_2$ NRs with weak Ir–Te bond strength exhibited excellent photothermal

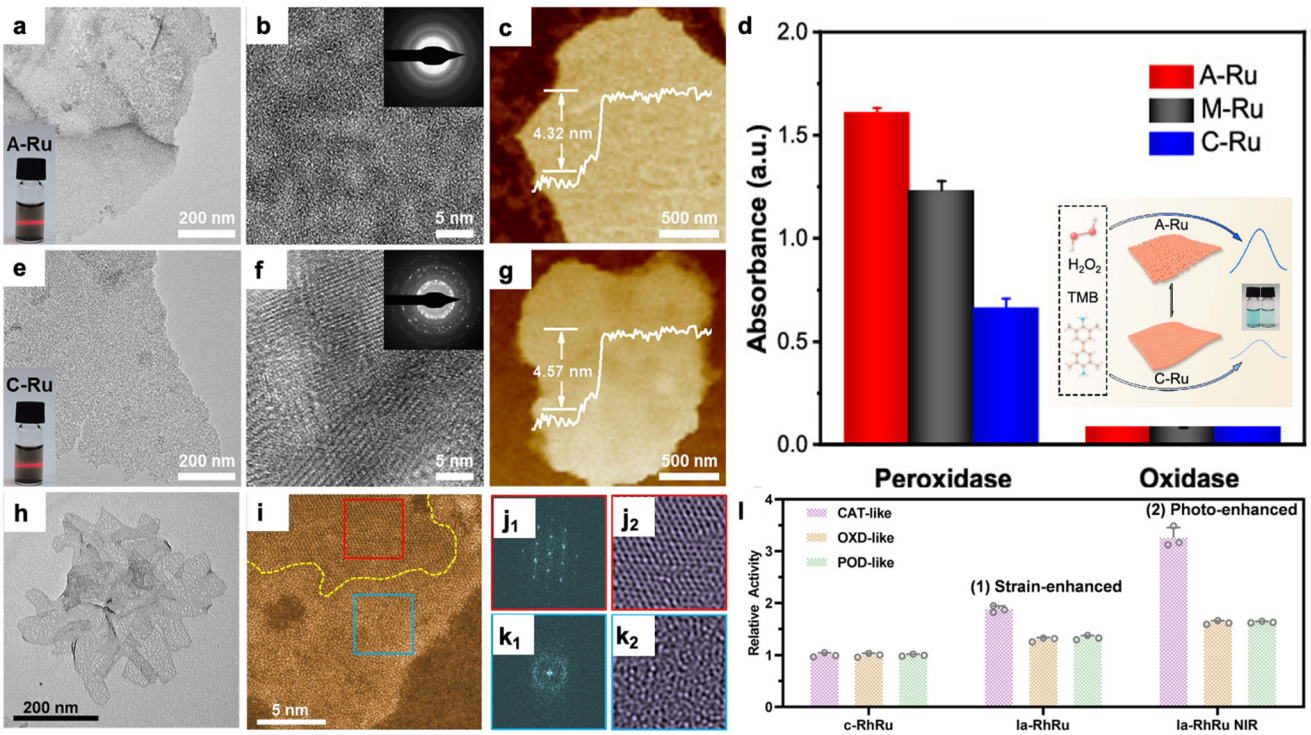

Fig. 5 TEM images of (a) amorphous Ru (A-Ru) and (e) crystalline Ru (C-Ru) nanosheets (NSs). Insets: digital photos of the corresponding aqueous solutions. HRTEM images of (b) A-Ru and (f) C-Ru NSs. Insets: the corresponding selected area electron diffraction (SAED) patterns. Atomic force microscope images of (c) A-Ru and (g) C-Ru NSs. (d) Comparisons of POD-like and OxD-like activity of Ru NSs with different degrees of crystallinity. Inset: schematic illustration of the POD-like activity of Ru NSs. Reproduced with permission from ref. 88. Copyright 2021, American Chemical Society (h) TEM image and (i) spherical aberration corrected (C_S-corrected) high-angle annular dark-field scanning TEM (HAADF-STEM) image of amorphous-crystalline heterophase RhRu NSs, with corresponding (j_1 and k_1) FFT patterns and (j_2 and k_2) HR-STEM images taken from the red and cyan squares in (i). (l) Comparisons of CAT-, OxD-, and POD-like activities of crystalline RhRu (c-RhRu) and amorphous-crystalline heterophase RhRu (denoted as la-RhRu) nanozymes, showing strain-enhanced effect and photoenhanced effect on enzymatic performances. NIR: near-infrared. Reproduced with permission from ref. 35. Copyright 2024, Wiley-VCH.

conversion efficiency and enzymatic performance. These properties could significantly contribute to synergistic oncotherapy, effectively achieving outstanding antitumor efficiency.[55]

Besides the fully amorphous phase, an amorphous–crystalline heterophase can also modify the surface properties and catalytic efficiency of noble metal-based nanomaterials. For instance, RuCu nanosheets composed of crystalline Ru and amorphous Cu exhibited a wider pH range for the oxidation of POD substrate H_2O_2 and demonstrated POD-like activity with high catalytic efficiency (K_{cat}/K_m = 177.2 m^{-1} s^{-1}).[19] Additionally, Guo *et al.* synthesized amorphous–crystalline heterophase PtRuTe nanomaterials with dominant amorphous phase, which consisted of a Pt/Te-enriched core and a Ru-enriched shell.[23] Compared with its less amorphous PtRuTe and fully crystalline PtRuTe counterparts, the highly amorphous PtRuTe could efficiently accelerate the oxidation of TMB by H_2O_2, indicating excellent POD-like activity. The authors supposed that enriched catalytically active sites as well as the electron redistribution induced by amorphous structure and multiple contents promoted the excellent POD-like property of the highly amorphous PtRuTe. Moreover, Wu *et al.* synthesized a heterophase RhRu bimetallene nanozyme (Fig. 5h–k).[35] Compared with crystalline RhRu, the amorphous–crystalline heterophase RhRu bimetallene possessed strong ultraviolet-visible (UV)-NIR absorption in a broad spectral range, leading to an exceptional intrinsic photothermal effect and photoenhanced CAT-, OxD-, and POD-like activities (Fig. 5(l)).[35]

2.1.5 Alloying. Alloying is regarded as one of the most promising methods for altering the catalytic properties of noble metals, as their electronic and geometric states can be adjusted by alloying with different elements.[59,96] To date, various strategies have been developed for synthesizing alloy nanocrystals, such as chemical co-reduction,[97,98] galvanic replacement,[99] seed-mediated synthesis,[100] and thermal decomposition.[101] Although noble metal-based alloys have been widely reported, few articles have systematically summarized the effects of alloying on nanozymes. Herein, the reported alloy nanozymes are further classified into random alloys, intermetallic alloys, and high-entropy alloys (HEAs).

2.1.5.1 Random alloy. Random alloys, also known as solid-solution alloys, feature a random distribution of atoms throughout the lattice.[102] Compared with monometallic nanozymes, multi-metallic alloy nanozymes can achieve improved chemical stability and enzymatic activity. For example, Meng *et al.* recently synthesized a AuPd alloy nanozyme with enhanced SOD- and myeloperoxidase-like activities compared with its pure Au and Pd counterparts. Furthermore, the enzymatic activities of the AuPd alloy nanozymes remained stable over a wide temperature range from 25 to 80 °C, indicating their high stability.[46] Additionally, several studies have confirmed that the enhancement of enzyme-like activities results from the electronic state modification of the active metal through alloying.[103–106] For example, Yan *et al.* doped a p-block metal Sn into Pd nanocrystals and investigated the enzymatic behaviors of PdSn nanozymes.[105] The energy dispersive spectroscopy (EDS) mappings demonstrated a homogeneous distribution of Sn and Pd (Fig. 6a). Projected density of states (PDOS) analysis indicated strong p–d orbital hybridization with the peaks of Pd 4d orbitals matching well with Sn 5p orbitals (Fig. 6b). The authors explained that the orbital hybridization could raise the d-band energy level, reducing antibonding electron filling and enhancing substrate adsorption. Consequently, PdSn nanozymes exhibited excellent POD-like activity with high V_{max} values for both H_2O_2 and TMB compared with pure Pd nanozymes. Furthermore, the PdSn nanozymes exhibited outstanding catalytic specificity (Fig. 6c). The activation energy calculated from the Arrhenius equation was used to demonstrate the enzyme-like performance. The PdSn nanozymes showed an activation energy value of 1.03 kJ mol^{-1} for POD-like activity and −4.64 kJ mol^{-1} for OxD-like activity, which illustrated the excellent specificity. Additionally, introducing functional compositions into noble metals can lead to the formation of a multifunctional nanoalloys with intriguing properties.[107] For example, oxophilic metals, such as Bi, Sn, and Ni, are widely incorporated into noble metals to enhance enzymatic activities by forming oxygen-containing species on the catalyst surface.[108,109] Xia *et al.* reported that the POD-activity of bimetallic PdBi alloy was closely correlated with Bi content on the surface, which was beneficial for strong adsorption of H_2O_2 on Bi and had a low potential barrier for further decomposition.[108] Similarly, the oxophilic metal Sn has been studied in a bimetallic PtSn nanozyme, where oxygen vacancy sites provided by SnO_{2-x} enhanced H_2O_2 adsorption, further boosting enzymatic activities to catalyze H_2O_2 into O_2 and hydroxyl radical ($^{\bullet}OH$).[109]

2.1.5.2 Intermetallic alloy. Intermetallic alloys refer to solid-state metallic alloys with an ordered atomic arrangement, which can lead to significant changes in their catalytic performance.[110–114] Recently, Zhu *et al.* reported a high-indexed intermetallic Pt_3Sn nanozyme with high activity and specificity, synthesized by a one-step solvothermal approach.[13] The lattice spacing of 0.283 and 0.179 nm could be assigned to (110) and (210) crystal planes of Pt_3Sn, respectively, confirming the formation of a high-indexed Pt_3Sn intermetallic structure (Fig. 6d and e). Consequently, the high-indexed Pt_3Sn (H-Pt_3Sn) exhibited the highest absorbance of ox-TMB at 371 and 652 nm compared with Pt_3Sn cubic and Pt nanozymes, indicating its superior POD-like activity (Fig. 6f). As expected, the H-Pt_3Sn demonstrated approximately twice the specific activity value (345.32 U mg^{-1}) compared with that of Pt nanozymes (190.12 U mg^{-1}). In another work, Pd_2Sn intermetallic NRs were identified as multifunctional nanozymes for antitumor immunity.[115] In addition to enhancing catalytic activity, the Pd_2Sn intermetallics were further functionalized with soybean phospholipid and glucose oxidase (GOx), demonstrating a uniform hydrated particle size over 7 days in phosphate buffer, which indicated excellent stability. Notably, Pd_2Sn intermetallic NRs, featuring a plasmonic Pd component, exhibited high light absorption and photothermal conversion efficiency, making them suitable contrast agents for PAI due to the LSPR effect.

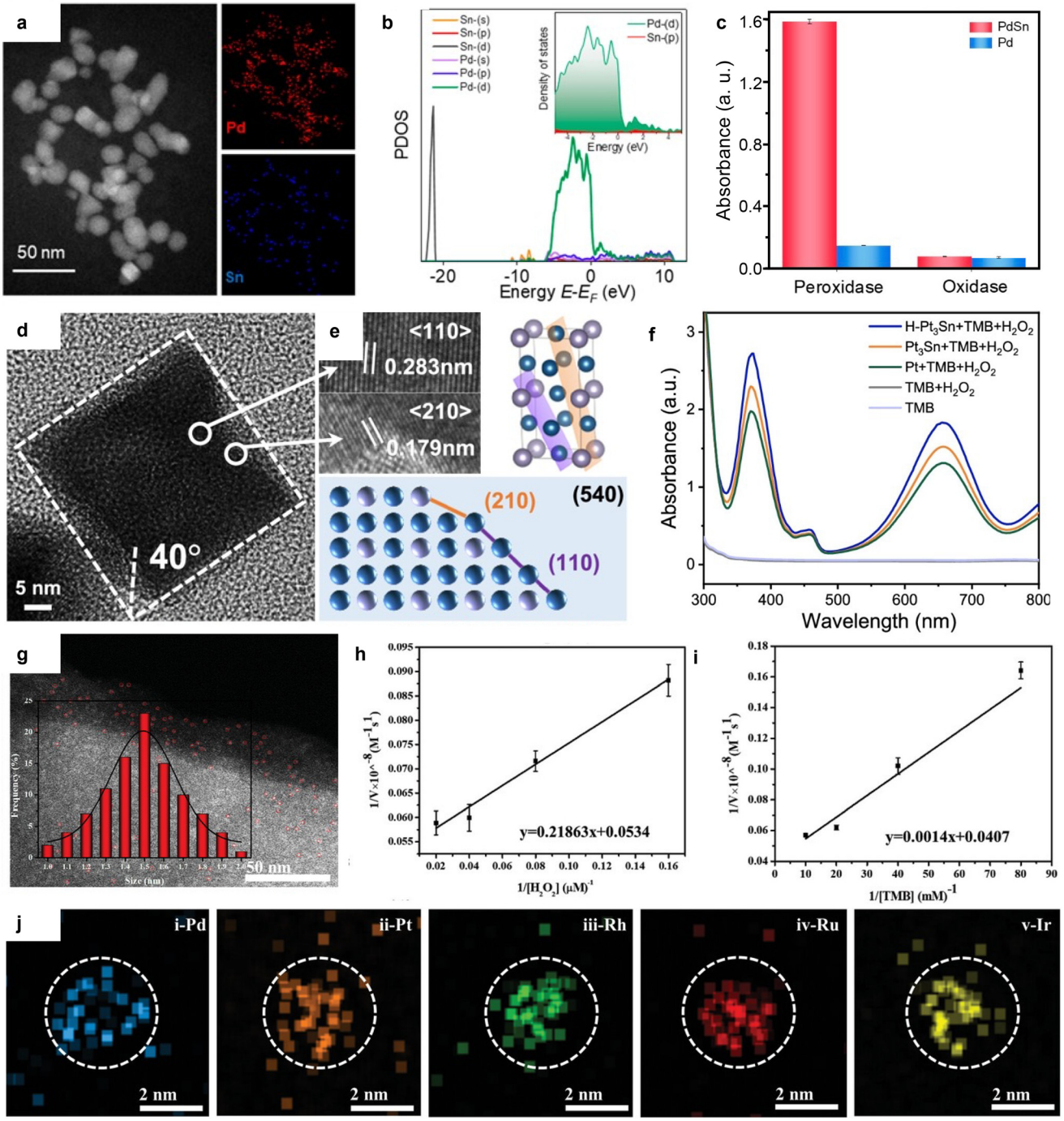

Fig. 6 (a) TEM image and energy dispersive spectroscopy (EDS) mapping of PdSn nanozymes. (b) Calculated projected density of state (PDOS) of PdSn nanozymes. Inset: calculated density of states of Pd 4d and Sn 5p orbitals. (c) Comparison of POD-like and OxD-like activities of Pd and PdSn nanozymes. Reproduced with permission from ref. 105. Copyright 2024, American Chemical Society. (d) HRTEM image of high-indexed Pt_3Sn (H-Pt_3Sn) intermetallic nanozymes. (e) The derived structure models and corresponding 2D atomic models of H-Pt_3Sn intermetallic nanozymes. (Pt: blue balls; Sn: gray balls). (f) Comparison of absorbance spectra (indicating the POD-like activities) of H-Pt_3Sn, Pt_3Sn, and Pt nanozymes, in which 3,3′,5,5′-tetramethylbenzidine (TMB) was used as the substrate to catalyze H_2O_2. Reproduced with permission from ref. 13. Copyright 2022, American Chemical Society. (g) STEM images of the ultra-small PtPdRuRhIr high-entropy alloy nanoparticles (US-HEANPs) (inset: size distribution of US-HEANPs). Steady-state catalytic kinetics of POD-like activities of high-entropy alloy nanozymes with different concentrations of (h) H_2O_2 and (i) TMB, revealing the fast POD-like reaction rate and strong affinity between nanozymes and substrate. (j) EDS mapping of US-HEANPs. Reproduced with permission from ref. 121. Copyright 2023, Wiley-VCH.

2.1.5.3 High-entropy alloy. To date, HEAs have demonstrated tremendous potential in energy, engineering, catalysts fields.[116–118] Compared with traditional alloys, HEAs consist of five or more principal elements in nearly equal percentages, typically ranging from 5 to 35 at%.[118,119] The variable element compositions of HEAs offer greater flexibility in adjusting the coordination environment, thereby optimizing reaction activities. On the other hand, the high mixing entropy of HEAs contributes to the stability of the material system.[120] Recently, HEAs have also been applied in the field of nanozymes.[121–123] Ai *et al.* prepared ultra-small PtPdRuRhIr high-entropy alloy NPs by a general metal–ligand cross-linking strategy.[121] These HEANPs have an average size of approximately 1.5 nm and consist of Pt, Pd, Ru, Rh, and Ir (Fig. 6g and j). The POD-like activities of high-entropy alloy nanozymes (HEAzymes) with H_2O_2 and TMB were observed with a small K_m value and high V_{max}, indicating their exceptional POD-like activity (Fig. 6h and i). The authors claimed that the presence of random mismatches and occupancies of five different atoms in the alloys could accelerate the transfer of electrons by HEAzymes, which may contribute to their high enzymatic performance. Additionally, the slow diffusion effect of HEAs and the increased mixed conformational entropy contributed to the excellent stability of PtPdRuRhIr HEANPs. Beyond noble metal-dominant HEAs, FeCuAgCeGd HEAzymes[122] and MnFeCoNiCu HEAzymes[123] have also been reported recently.

2.1.6 Ligand. Ligand modification is an effective strategy for improving catalytic activity, changing chemical selectivity or even altering enzyme-like behaviors of nanozymes, presumably due to steric effects,[124,125] adsorption interactions between the substrate and the ligand,[126] or charge transfer between the ligand and surface atoms.[127] A recent study investigated the effects of several commonly used ligands, including poly(vinyl pyrrolidone) (PVP), polystyrene sulfonate (PSS), poly (vinyl alcohol) (PVA), and poly(acrylic acid) (PAA), on the POD-like activity of Ru nanozyme (Fig. 7a).[51] Notably, Ru@PSS showed the most enhanced POD activity through charge transfer between ligand and Ru atoms. The electronic properties of the Ru nanozymes were characterized by X-ray photoelectron spectroscopy (XPS), which revealed that the extent of the charge transfer was in the following order: Ru@PSS > Ru@PVA > Ru@PVP > Ru@PAA (Fig. 7b). As a result, Ru@PSS exhibited the highest POD-like activity, with a specific activity of 2820 ± 130 U mg^{-1}, which was approximately fivefold times that of Ru@PAA (521 ± 52 U mg^{-1}) (Fig. 7c). DFT calculation results further verified the role played by ligands. Specifically,

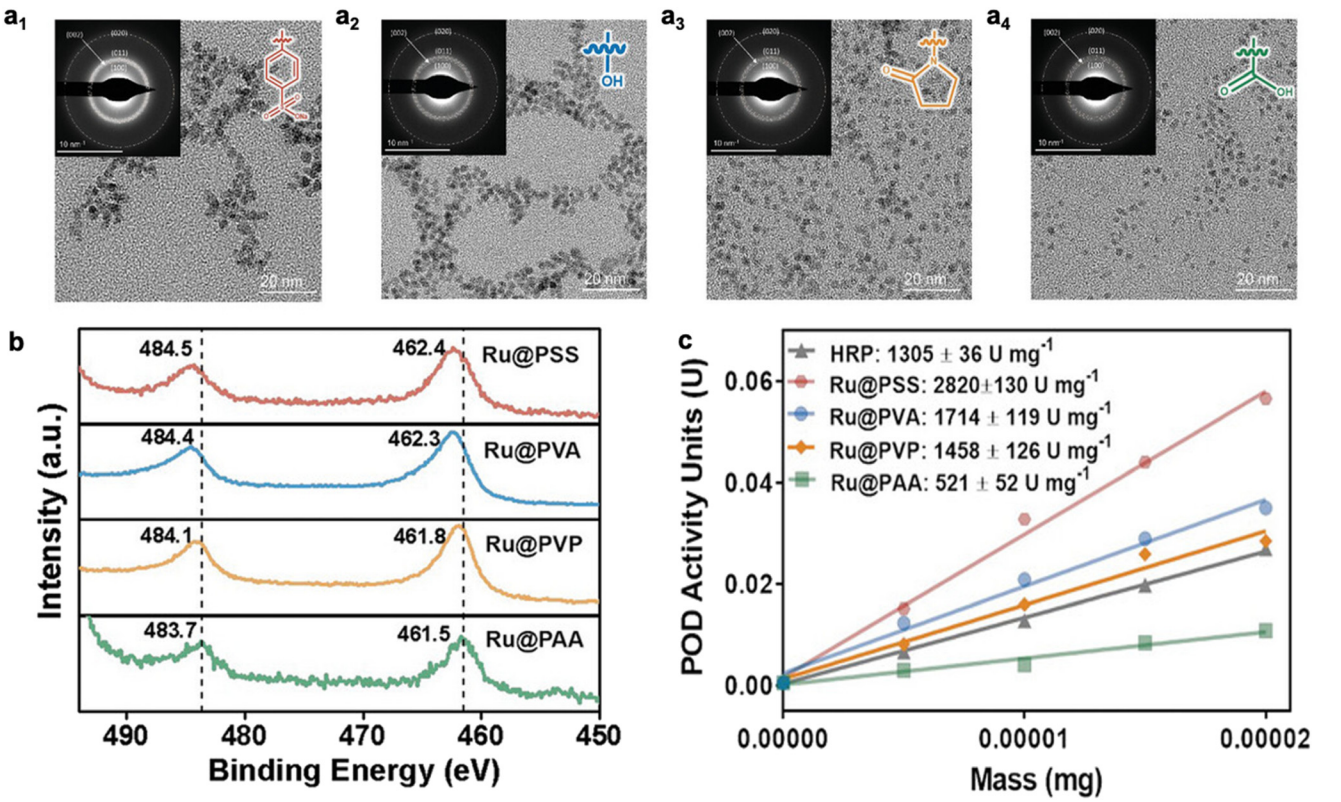

Fig. 7 (a) TEM images of Ru NPs modified with different ligands, including polystyrene sulfonate (PSS) (a_1), poly(vinyl pyrrolidone) (PVP) (a_2), poly (vinyl alcohol) (PVA) (a_3), and poly(acrylic acid) (PAA) (a_4). Insets: the corresponding SAED patterns of Ru NPs with PSS ligands (Ru@PSS), Ru NPs with PVA ligand (Ru@PVA), Ru NPs with PVP ligand (Ru@PVP), and Ru NPs with PAA ligand (Ru@PAA). (b) High-resolution X-ray photoelectron spectroscopy spectra of Ru 3p for Ru@PSS, Ru@PVA, Ru@PVP, and Ru@PAA nanozymes, respectively. (c) The specific activities (U mg^{-1}) of horseradish peroxidase (HRP) and various Ru nanozymes, among which Ru@PSS exhibits the highest slope (POD-like activity) in the linear fitting curves. Reproduced with permission from ref. 51. Copyright 2023, Wiley-VCH.

Ru@PSS exhibited weaker adsorption of ˙OH and smaller reaction energies for TMB oxidations compared with Ru@PAA nanozymes. Besides enhanced activity, ligand modification could also impart substrate specificity of nanozymes.[56] For example, Li *et al.* modified Pt NPs with various sulfide surface ligands, including 1-adamantane mercaptan, methyl thioglycolate, 6-mercapto-6-deoxybeta-cyclodextrin, sodium 2-mercaptoethane sulfonate, β-mercaptoethanol, and mercaptoacetic acid, to enhance their OxD-like performance.[56] When taking TMB as the substrate, all functionalized Pt NPs demonstrated higher OxD-like activity compared with bare Pt NPs. Specifically, the Pt NPs modified by 6-mercapto-6-deoxybeta-cyclodextrin exhibited a K_{cat}/K_m value 3.4 times that of bare Pt NPs. Remarkably, it was found that the enzymatic performance of these functionalized Pt NPs toward alternative substrates such as 2,2′-azino-bis(3-ethylbenzo-thiazoline-6-sulfonic acid) diammonium salt and *o*-phenylenediamine remained unchanged, suggesting a substrate selectivity to the functionalized Pt nanozymes. Additionally, through ligand engineering, the target enzymatic reaction of a nanozyme can be directly altered. Lin *et al.* reported that citrate-modified Au NPs displayed glucose OxD-mimetic activity, while cysteine-modified Au NPs exhibited POD-like activity, illustrating that ligand type can directly determines the enzyme-like behaviors of nanozymes.[128] Moreover, the ligand effect also works on nanoclusters.[129,130] For instance, a bioinspired surface ligand engineering was achieved by integrating the POD cofactor Fe (III) *meso*-tetra(4-carboxyphenyl)porphine (Fe-TCPP) onto the surface of glutathione-stabilized Au nanoclusters (AuSG). The resulting AuSG-Fe-TCPP clusterzymes showed a 39.6-fold enhancement in POD-like activity compared with AuSG.[129] These studies suggest that ligand engineering is a powerful approach for modulating the behaviors of noble metal nanozymes for more sensitive and specific applications.

2.2 Structural engineering of noble metal-based nanozyme heterostructures

Construction of heterostructures based on noble metal nanozymes can effectively enhance their dispersity and stability during storage and catalysis, while the presence of various heterostructure interfaces may promote electron transfer and change atomic coordination environments, thereby further regulating the enzyme-like behaviors.[6,131,132] Meanwhile, the incorporation of multiple components in the nanozymes endow them with more possible functions for integrated applications such as synergistic therapy,[133–135] theragnostic agents for both diagnosis and therapy,[45] as well as multiple imaging modalities.[21] Herein, we discuss the construction of various heterostructures based on noble metal nanozymes with the addition of different second components, including metals, metal compounds, carbon materials, metal–organic frameworks (MOFs), covalent–organic frameworks (COFs), *etc*.

2.2.1 Noble metal–noble metal heterostructures. Several studies have demonstrated that constructing metal–metal heterostructures, such as core–shell, Janus, and satellite structures, can modulate the surface properties and electronic structure of nanozymes, leading to tunable substrate adsorption behaviors and significantly improved catalytic activity. For instance, a POD-like nanozyme with Ni-rich core and Pt-rich shell (Fig. 8a–c) exhibited a high catalytic efficiency with K_{cat} of 10^7 s^{-1} to TMB oxidation.[52] Compared with Pt NPs, the core–shell heterostructure with a Ni/Pt atomic ratio of 1/1 demonstrated an improved POD-like activity (Fig. 8d–f). The authors attributed this enhancement to the Ni-rich core, which shifted the d-band center of the Pt shell downward. This shift weakened the adsorption of HO*/O* (key oxidant species generated during H_2O_2 decomposition) on the Pt surface, facilitating the transfer of these oxidant species to the TMB substrate. As a result, the core–shell heterostructure nanozyme demonstrated a significantly improved catalytic activity with 46-fold increase in K_{cat}. In another work, Wang *et al.* synthesized trimetallic dendritic nanozymes (Pd@Pt–Ru, Fig. 8g–i) with a K_m value of 5.23 mM for H_2O_2 detection.[20] XPS results revealed that the Ru deposition on the PdPt core induced electron transfer from Pd and Pt to Ru. On the one hand, the electron-deficient PdPt enhanced its interaction with the TMB substrate. On the other hand, the reduced electron density of Pt lowered the energy barrier for H_2O_2 decomposition, thereby improving POD-like activity. In contrast, Au deposition caused electron transfer toward Pd and Pt, resulting in decreased catalytic activity (Fig. 8i).

Plasmonic metal-based heterostructure nanozymes are another representative group of nanozyme heterostructures that have attracted significant attention due to their unique photoresponsive properties.[32] The decay of LSPR from a plasmonic metal can induce the near-field enhancement and generate hot carriers (hot electrons and hot holes) and local heating (photothermal effect), which could be utilized by adjacent components to extend their free path and enhance their lifetime and efficiency.[135] For example, Sang *et al.* designed a Pd–Au dimer with a clear boundary and independently exposed Pd and Au surfaces.[136] Under light irradiation, the TMB oxidation capability of the Pd–Au dimer increased by 2.3 times compared with dark conditions. After excluding the photothermal effects, the authors attributed the catalytic activity enhancement to the LSPR effect of Au. Specifically, LSPR-induced electron–hole pairs in Au were transferred to Pd, facilitating the decomposition of H_2O_2 on the Pd surface into reactive oxygen species (ROS) including ˙OH, $^{\cdot}O^{2-}$ and $^1O_2$. A different work studied the local photothermal effect of heterostructures induced by LSPR excitation, which could also regulate the enzyme-like performance.[132] Fan *et al.* synthesized plasmon-enhanced OxD-like rod-shaped nanozymes with Pd coating and Au core (Au@PdNRs).[132] Under 808 nm irradiation (close to the LSPR absorption wavelength of Au NRs), the catalytic performance of Au@PdNRs was significantly enhanced. Based on the slight change in the activation energy of Au@PdNRs before and after irradiation, the authors suggested that the contribution of hot electrons to the activity enhancement was minimal and the primary contribution came from the local photothermal effect induced by LSPR. The advantages of plasmonic metal-based heterostructure nanozymes

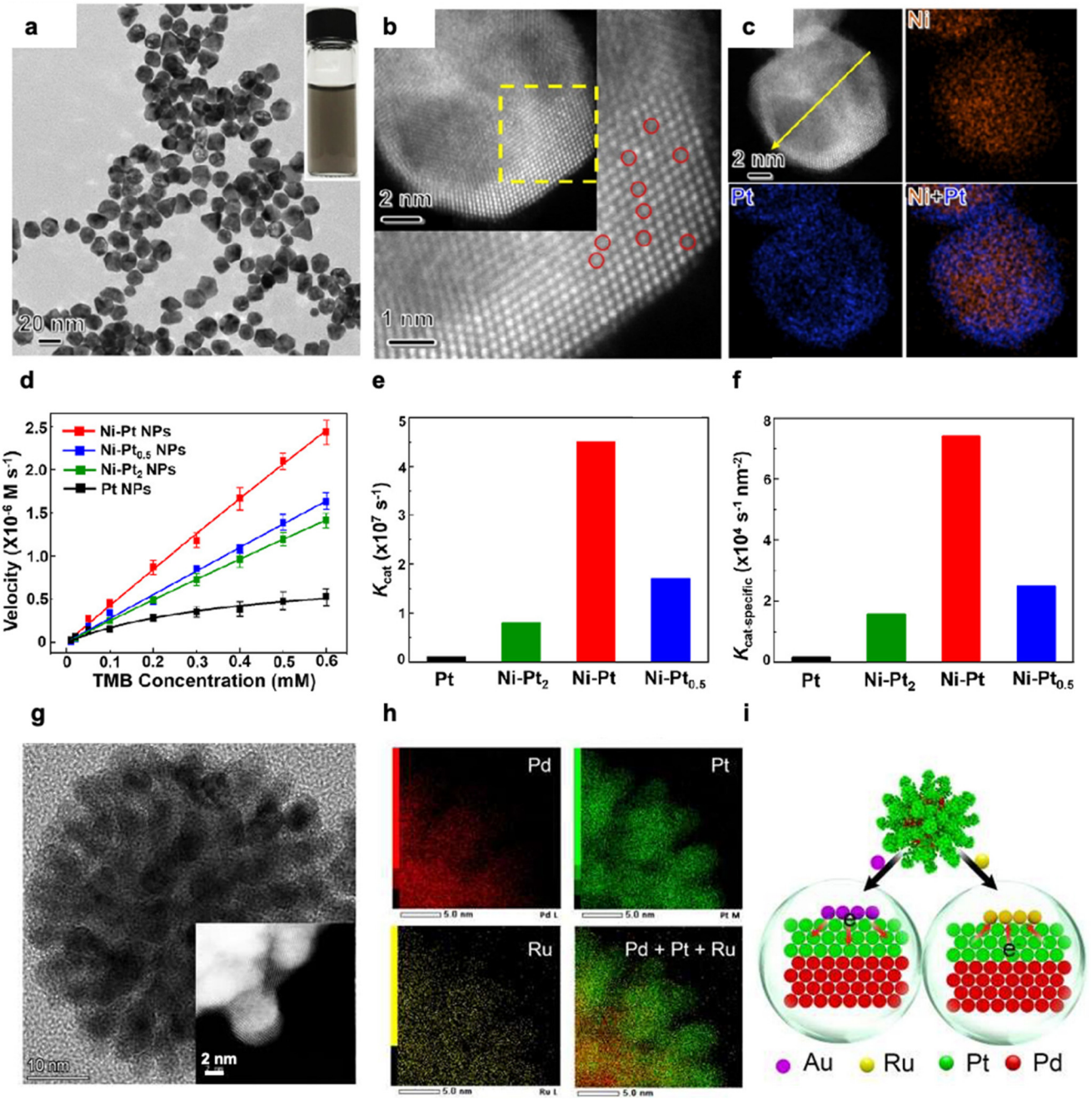

Fig. 8 (a) TEM image of Ni–Pt NPs and photograph (inset) of the aqueous suspension. (b) HAADF-STEM image of a typical Ni–Pt heterostructure. Red circles highlight regions containing Ni atoms. (c) EDS mapping of Ni–Pt NPs showing Ni-rich core and Pt-rich shell. (d–f) POD-like catalytic efficiencies for Ni–Pt NPs with different Ni/Pt ratios. (d) Plots of initial reaction velocity against TMB concentration, (e) K_{cat} (catalytic constant) values, and (f) $K_{cat\text{-}specific}$ (K_{cat} normalized to the surface area) values of different Ni–Pt NPs. The NPs with Ni/Pt ratio of 1 : 1 exhibited the highest catalytic activity. Reproduced with permission from ref. 52. Copyright 2021, American Chemical Society. (g) HRTEM images and (h) EDS mapping of Pd@Pt–Ru nanozyme. (i) Scheme of electron migration in Pd@Pt–Au and Pd@Pt–Ru NPs. The Ru deposition on PdPt core induces electron transfer from Pd/Pt to Ru, whereas the Au deposition induces electron transfer toward Pd and Pt. Reproduced with permission from ref. 20. Copyright 2024, American Chemical Society.

have also been demonstrated in other enzyme-mimicking reactions. For example, Pt-tipped Au NRs exhibited excellent CAT-like performance under NIR light irradiation,[133] $Au@Pt_{0.46}Ag_{0.54}$ nanozymes displayed enhanced CAT-, OxD-, and POD-like activities alongside efficient photothermal conversion under an 808 nm laser,[131] while 2D Pd@Au core–shell nanosheets demonstrated robust CAT-like activity by stably producing O_2 under NIR-II laser excitation.[41] Due to their outstanding catalytic and optical properties, plasmonic nanozymes have found extensive applications in advanced synergis-

tic therapeutic methods, such as photodynamic and photothermal therapy.[12,40,134]

2.2.2 Noble metal–metal compound heterostructures. Incorporating metal compounds, such as oxides,[137,138] sulfides,[139] phosphides[140] and carbides,[141] with noble metal-based nanozymes can improve their dispersion and enable cascade catalysis. For example, ultrasmall Ir/$WO_{2.72}$ nanocomposites as POD mimics exhibited excellent area-specific catalytic efficiency of 1.5×10^4 s^{-1} nm^{-2}, which is comparable for most noble metals.[17] The ultrasmall size of Ir NPs (~1.1 nm) that results in exceptionally high catalytic efficiency could be well preserved on the oxide support, in which the high hydrophilicity of $WO_{2.72}$NRs effectively prevented aggregation of the ultrasmall Ir NPs. In another study, a CeO_2/Pt heterostructure nanozyme was synthesized within zwitterionic vesicles and utilized to mimic the peroxisome for ROS detoxification.[142] CeO_2 exhibited SOD-like catalytic activity, while Pt demonstrated CAT-like activity. As a result, the heterostructure successfully displayed cascade catalytic activity, converting superoxide radicals ($O_2^{\bullet-}$) into H_2O_2 followed by transforming H_2O into O_2.

In addition, metal compounds with unique physicochemical properties bring new functions to the noble metal nanozymes. For example, Fe_3O_4 is a typical magnetic and recyclable material that can be used in magnetic resonance imaging and magnetic thermal therapy. He *et al.* synthesized monodisperse Fe_3O_4-Au@mesoporous SiO_2 microspheres with cascade catalytic ability.[143] The superparamagnetic Fe_3O_4 cores not only benefitted from POD-like activity but also enabled a recyclable enzymatic system. Combined with the GOx-like activity of Au, the catalyst achieved cascade catalytic activity from glucose oxidation to TMB oxidation. Different from Fe_3O_4, Ti_3C_2 nanosheets were found to possess high absorption in the NIR-II range and are thus excellent materials for PTT. A $Ti_3C_2T_x$-Pt-PEG heterostructure nanozyme was synthesized by anchoring Pt NPs with POD-like activity onto Ti_3C_2,[141] which achieved synergistic cancer cell killing under low-energy density NIR-II laser irradiation through both photothermal effects and enzyme-like catalysis. Additionally, due to the excellent optical absorption of Ti_3C_2, this integrated nanozyme could also serve as PAI agent to accurately display the treatment site, facilitating imaging-guided synergistic cancer therapy. Similarly, a PtFe@Fe_3O_4 heterostructure nanozyme constructed by Li *et al.* also exhibited the ability to kill tumor cells through the synergistic effect of photothermal and enzymatic therapy.[101] The authors believed that redistribution of electrons in each component enhanced the POD-like activity of Pt and the CAT-like activity of Fe^{3+}, while the photothermal effect shared by both Pt and Fe_3O_4 enabled the PTT and PAI functionalities. In another work, a heterostructure nanozyme assembled from zinc phthalocyanine, Pt, and the semiconductor TiO_2 also demonstrated synergistic activities in enzyme catalysis, PDT, and PTT.[144]

2.2.3 Noble metal–carbon heterostructures. Carbon materials have attracted extensive attention in biomedical applications because they are considered a physical analogue of extracellular matrix components.[145] Integrating carbon materials with noble metals is an efficient method to enhance the dispersion and biocompatibility of noble metal-based nanozymes and simultaneously adjust the catalytic properties by tuning the charge transfer and substrate adsorption behaviors at the metal–carbon interface.[146,147] For instance, Liang *et al.* reported a multifunctional POD-like nanozyme based on the assembly of carbon dots (CDs) and Pt NPs for versatile diagnosis and therapy of pathogen infections.[148] The introduction of CDs not only provided red fluorescence as a probe for specific fluorescence assay of H_2O_2, but also shifted the d-band center of Pt NPs upwards, thereby enhancing the initial adsorption of H_2O_2 and promoting the cleavage of the O–O bond, ultimately improving the oxidation efficiency of the TMB. Zhang *et al.* developed another Pt@carbon nanodots (CNDs) nanozyme with SOD- and CAT-like activities by depositing Pt NPs on carbonyl and hydroxyl groups-rich CNDs.[149] The obtained Pt@CNDs nanozyme exhibited efficient cascade catalytic activity, in which the heterostructure nanozyme served as a SOD mimic to catalyze the dismutation of $O_2^{\bullet-}$ to H_2O_2 while the Pt NPs also mimicked CAT to catalyze the decomposition of H_2O_2 to produce H_2O. Thanks to the effectively promoted electron transfer and prevention of Pt NP aggregation by CNDs, the Pt@CNDs exhibited much higher catalytic activities compared with either Pt NPs or CNDs. Fan *et al.* reported yolk–shell gold@carbon nanospheres, which possessed excellent POD- and OxD-like activities and photothermal conversion properties.[150] The permeable carbon shells could prevent aggregation of Au NPs and allowed H_2O_2 as well as TMB to access Au NPs for effective enzyme-like catalytic reactions. Importantly, the enzyme mimicking activities could be enhanced by an 808 nm laser irradiation due to the photothermal effect of gold@carbon nanospheres.

2.2.4 Noble metal–MOF and noble metal–COF heterostructures. MOFs are crystalline framework materials featuring intramolecular pores and formed by self-assembly of metal ions or clusters and organic ligands through coordination bonds.[151,152] Since MOFs possess abundant active sites for binding noble metals and mimicking enzymatic activities, integration of MOFs with noble metal nanozymes has been proved effective for enhancing their catalytic activity and achieving cascade catalysis.[153] Huang *et al.* synthesized Au NPs/2D MOF hybrid nanosheets by growing ultra-small Au NPs on metalloporphyrinic MOF nanosheets.[154] These hybrid nanosheets served as nanozymes to catalyze enzymatic cascade reactions and detect glucose by combining the GOx-like activities of Au NPs with the POD-like activities of the MOF nanosheets. In another example, a SOD/CAT mimetic cascade nanozyme was prepared by loading Pt NPs onto Mn-modified MOFs (namely Pt@PCN222-Mn), where Pt NPs exhibited CAT-like activity and the Mn(III) porphyrin structures exhibited SOD-like activity.[155] This integrated nanozyme featured two spatially separated active sites that mimic SOD and CAT, while a confinement effect increased the mass-transfer efficiency and reduced the transfer time between catalytic centers. In addition to catalyzing cascade reactions, nanozyme–MOF

heterostructures could also be employed as bio-sensors. Liu *et al.* utilized a Ce-MOF modified with Pt NPs to create a novel nanocomposite, MVCM@Pt, for highly sensitive detection of visfatin.[156] Pt NPs served as carriers for amino-modified single-stranded DNA and co-catalysts for MVCM, endowing the nanocomposite with significantly high POD-like catalytic activity.

COFs, known for their consistent porosity and substantial carbon and nitrogen backbone, have also been effectively paired with noble metals to stabilize nanozymes.[157,158] For example, Liu *et al.* synthesized COFs with a hierarchical flower-like hollow structure and subsequently produced COF-Ag nanozymes through *in situ* reduction of Ag NPs on the COF.[159] They found that COFs, as carriers, could effectively regulate the dispersion and size of Ag NPs, thereby enhancing the catalytic stability of COF-Ag nanozymes. The COF-Ag nanozymes showed high sensitivity and selectivity in catalysis-based colorimetric detection of Hg^{2+} ions in blood due to the formation of the Ag–Hg metallic bond and the enhanced OxD-like activity of COF-Ag nanozymes in the presence of Hg^{2+} ions. Moreover, a Pt–Pd alloy/COFs nanozyme was obtained through a simple aldimine condensation and *in situ* reduction method.[160] This heterostructure provided abundant anchor sites for Pt–Pd bimetallic NPs, preventing the aggregation of Pt–Pd NPs, and enhancing both stability and activity in POD-like and OxD-like catalysis.

2.2.5 Other heterostructures. In addition to the heterostructures mentioned above, many other materials are recognized as excellent supports for noble metal nanozymes. For example, Sun *et al.* synthesized the Au–Pd/MoS_2 nanozyme by anchoring Au–Pd core–shell NPs on exfoliated MoS_2 nanosheets.[161] This hybrid, with an Au/Pd mass ratio of 1 : 2 ($Au_{1.0}Pd_{2.0}/MoS_2$), demonstrated synergistically enhanced POD-like activity due to strong metal–metal and metal–support interactions. In another example, by immobilizing Au NPs on hollow silica microspheres (HSM), the obtained HSM-AuNPs possessed dual enzymatic (GOx and POD-like activities) activity to promote the cascade reactions.[162] The HSMs not only enabled Au to be uniformly anchored, exposing more active sites, but also assisted in the diffusion of reaction substrates and products, thereby enhancing the stability of the reaction environment.

Different from the above examples, carbon nitride (C_3N_4) can not only improve the dispersity of nanozymes, but also act as POD mimics by themselves.[163] Ding *et al.* prepared highly dispersed ultrasmall Ru NPs anchored onto C_3N_4 nanosheets for colorimetric detection. With excellent carrier capability, p-conjugated framework and the abundant pyridinic nitrogen, the C_3N_4 support provided uniform binding sites for Ru NPs, thereby promoting their POD-like catalytic performance.[164] Au NPs grown on the surface of C_3N_4 have also been reported to show an excellent improvement in POD-like activity.[165] Benefiting from the synergistic effect of Au NPs and g-C_3N_4 nanosheets, the catalytic activity of the AuNPs@g-C_3N_4 nanosheets was 6 times that of the physical mixture of naked AuNPs and g-C_3N_4 nanosheets.[165] In addition, other noble metals such as Pt[166] and Ag[167] have also been used to construct heterostructures with C_3N_4 nanosheets for nanozyme applications.

Single-atom based nanoheterostructures have emerged as another promising nanozyme candidate.[168–171] With optimized atomic utilization efficiency and strong metal–support interactions, the enzyme-like activity of active sites in SAzymes could be precisely regulated in terms of the coordination environment and charge transfer.[168,169] Chang *et al.* developed a nitrogen-coordinated carbon-supported Pd SAzyme by pyrolyzing Pd NPs supported on MOFs.[172] The developed SAzyme exhibited excellent POD-like activity as well as a glutathione oxidase-like activity, which reduced overproduced intracellular glutathione in cancer cells. By limiting glutathione, the SAzyme effectively prevented the depletion of $^{\bullet}OH$, a key product of the POD-like reaction. Combined with the photothermal effect, the Pd SAzyme demonstrated effective PTT with mild treatment conditions. SAzymes have also shown promise in PDT. For example, Wang *et al.* partially replaced Co in $Mn_3[Co(CN)_6]_2$ MOFs with Ru to synthesize an SAzyme containing Ru single-atom sites.[173] The authors proposed that the six unsaturated Ru–C_6 coordination sites in SAzymes enhanced enzyme-like activity, enabling the rapid decomposition of H_2O_2. Furthermore, due to coordination and other noncovalent interactions, this SAzyme could self-assemble with the chlorin e6 photosensitizer, releasing highly cytotoxic $^1O_2$ species to enable PDT. Additionally, Yan *et al.* reported a Pt SAzyme-based bandage for brain trauma.[174] By reducing Pt onto CeO_2 clusters, they doped single-atom Pt in CeO_2 with a 2% lattice expansion of CeO_2. The Pt SAzyme exhibited glutathione peroxidase-like activity along with 10 times higher POD-like activity, 10 times higher CAT-like activity, and 4 times higher SOD-like activity compared with CeO_2 clusters. The Pt SAzyme was then incorporated into a bandage for noninvasive brain trauma treatment, which could prevent neuronal damage by effectively reducing reactive oxygen and nitrogen species.

3. Enzyme-like catalytic behaviors of noble metal-based nanozymes

In this section, we will introduce representative enzyme-like processes in which noble metal-based nanozymes have been applied and studied. Their enzyme-like catalytic behaviors including substrate adsorption, electron transfer, and product release in specific catalytic processes will be discussed.

3.1 POD

The POD family is the most common type of enzyme present in virtually all living species, and includes peroxidase, glutathione peroxidase, and haloperoxidase.[4] A typical reaction catalyzed by POD mimics, using TMB as substrate for the oxidation of H_2O_2, can be written as follows:[175]

$$H_2O_2 + 2TMB + 2H^+ = 2H_2O + 2TMB^+$$
(oxidized form of TMB)

In 2010, cysteamine-encapsulated Au NPs were unexpectedly discovered as mimics of POD for the oxidation of H_2O_2.

Since then, the POD-like behaviors of noble metal-based nanozymes have been further explored.[24] He *et al.* reported that the absorbance peak of Au NPs in UV-vis spectra remained unchanged during the POD-like reaction, indicating that Au NPs acted as the catalyst rather than the reactant.[176] Furthermore, several studies demonstrated that the intermediate $^{\bullet}OH$ was observed during the catalytic reaction when noble metal-based nanomaterials were used as POD mimics.[72,177] Mechanism studies showed that the adsorption of H_2O_2 on Au, Ag, Pd, and Pt is the first step to initiate the reaction. The predicted pathway is that H_2O_2 first breaks the O–O to form two OH* ('*' is utilized to indicate adsorbed species on the metal surface), followed by the formation of H_2O^* and O*, or alternatively the formation of H*, O* and OH*.[178] Recently, Shen *et al.* calculated the adsorption energy of OH* *via* DFT, which showed that the hydroxyl adsorption energies of Au, Ag, Pt, Pt, Ir, Rh, and Ru were located within the POD-like activity window, predicting their good POD-like activity.[179] This theoretical prediction matched well with the currently experimental confirmation of POD activities of noble metals.

3.2 OxD

OxD-like nanozymes exhibit a chemical catalytic function similar to oxidases, promoting the oxidation process of organic substrates such as TMB, glucose, glutathione, ascorbic acid, and 2,2′-azino-bis(3-ethylbenzothiazoline-6-sulfonic acid).[180] Taking TMB as an example, two possible enzyme-driven oxidation reactions of TMB are written as follows:[175]

$$O_2 + 2TMB + 2H^+ = H_2O_2 + 2TMB^+$$

$$O_2 + 4TMB + 4H^+ = 2H_2O + 4TMB^+$$

Unlike POD-like nanozymes, OxD-like nanozymes produce H_2O_2 with O_2 by acting as the hydrogen acceptor for substrate oxidation.[68,172,181–184] Long *et al.* demonstrated the oxidation reactions of TMB with Pd NPs as the OxD mimics, finding that O_2 could be adsorbed on the surface of Pd NPs and subsequently activated into O_2^1 through electron transfer from metal atoms to O_2.[183] Subsequent reports have identified several ROS in OxD-like processes, including $^{\bullet}OH$,[39] $^1O_2$ [185] and $O_2^{\bullet-}$,[183] which promote the oxidation of various substrates. Furthermore, Shen *et al.* investigated the catalytic mechanism of noble metal OxD-like nanozymes through a combination of DFT calculations and experimental investigations.[74] They proposed that noble metal nanomaterials facilitated the dissociation of O_2, producing O adatoms that subsequently could oxidize substrates (such as TMB and ascorbic acid) by extracting hydrogen from substrates.[74] Additionally, it is worth noting that noble metal-based nanozymes have also been utilized in other reactions in the OxD family. For instance, Chen *et al.* studied the catalytic mechanism of noble metal nanozymes as glucose oxidase, showing that Au NPs can catalyze glucose oxidation by reducing glucose to H_2O_2, while Pt, Pd, Ru, Rh, and Ir can preferentially reduce O_2 to H_2O.[186] Moreover, reports showed that PdPtCu nanocomposite, Pt NPs, and Pt/CeO_2 nanozyme can act as glutathione oxidase,[11] ascorbate oxidase,[187] and uricase mimics,[188] respectively. These findings broaden the types of OxD mimics achievable by the noble metal-based nanozyme family.

3.3 CAT

CAT-like nanozymes catalyze the decomposition of H_2O_2 according to the following reaction:[25]

$$2H_2O_2 = 2H_2O + O_2$$

O_2 can be effectively produced with CAT-like nanozymes, which are widely applied in overcoming tumor hypoxia.[25,27,189] In 2009, AuPt NPs stabilized with pectin were reported to exhibit CAT-like properties, which can decompose H_2O_2 to produce O_2.[190] Furthermore, Li *et al.* investigated the enzymatic performance mechanisms of Ag, Au, Pd, and Pt NPs.[178] In a basic environment, the CAT-like activity of noble metals involves H_2O_2 adsorbing onto the surfaces with pre-adsorbed OH groups, which then gives rise to H_2O^* and HO_2^*. Subsequently, HO_2^* reacts with another H_2O_2 to yield O_2^*, OH*, and H_2O^*. Interestingly, Ag, Au, Pd, and Pt NPs exhibit pH-switchable POD- and CAT-like activities. The authors claimed that pH value affects the reaction energy barriers and adsorption energies of noble metal NPs, resulting in POD-like activity at low pH and CAT-like activity at high pH, respectively. Indeed, the typical reaction condition of noble metal-based CAT-like mimics is a neutral or slightly alkaline environment, with commonly used buffers including phosphate buffer solution and sodium carbonate/sodium bicarbonate buffer solution.[191]

3.4 SOD

The SOD-like reaction for catalyzing $O_2^{\bullet-}$ can be written as follows:[31]

$$2O_2^{\bullet-} + 2H^+ = H_2O_2 + O_2$$

By clearing $O_2^{\bullet-}$ and generating O_2, SOD-like nanozymes effectively reduce oxidative stress in cells while mitigating apoptosis and inflammation.[31] Shen *et al.* utilized DFT calculations to predict the SOD-like activities of noble metals.[74] By analyzing the reaction pathway and energy changes on different noble metal surfaces, they proposed that $O^{2\bullet-}$ can easily capture protons from water, forming $HO_2^{\bullet}$ and OH^-. The adsorption of $HO_2^{\bullet}$ on the surfaces of Au, Ag, Pd, and Pt is a strongly exothermic process that occurs easily. Once $HO_2^{\bullet}$ is adsorbed on the noble metal surface, it readily converts to O_2^* and H_2O_2. Subsequently, O_2 and $H_2O_2^*$ are transformed into O_2 and H_2O_2. As a result, noble metals have great potential as SOD-like nanozymes.[74]

3.5 Multiple and specific enzyme mimics

Due to the high activity of noble metal nanomaterials in multiple enzyme-like reactions, most noble metal-based nanozymes exhibit two or more types of enzyme-like activities, enabling self-cascade synergistic catalysis.[192,193] For example, Li *et al.* constructed a PtFe@Fe_3O_4 nanozyme with dual POD–CAT enzyme-like activities, which could catalyze endogenous H_2O_2 to generate highly toxic $^{\bullet}OH$ and supply O_2, effectively

killing tumor cells and overcoming the tumor hypoxia.[101] In another work, by combining OxD-like activity to reduce O_2 to H_2O_2 with POD-like ability to consume H_2O_2 and produce $^{\bullet}OH$, Pd nanozymes could form a cascade catalytic system that produced abundant ROS.[72] It has been reported that the Pt@CNDs nanozymes with dual SOD–CAT activities could suppress oxidative damage by utilizing their SOD-like activity to clear $O_2^{\bullet-}$ and produce H_2O_2, as well as their CAT-like activity to decompose H_2O_2 into O_2.[149] Moreover, noble metal-based nanozymes with more than two enzyme-like activities have also been reported. For instance, a $AuPt_3Cu$ trimetallic nanozyme with Au-rich cores and Pt/Cu outer shells possessed OxD-, POD-, and CAT-like activities, displaying an excellent chemodynamic therapy performance towards cancerous MCF-7 cells without damage to normal cells.[6] Yang *et al.* synthesized ultrathin RuCu nanosheets that possessed POD-like activities, SOD-like activities and glutathione POD-like activities, demonstrating high catalytic efficiency in oxidizing H_2O_2 at a wide pH range and therefore their great potential as a chemodynamic therapy reagent.[19]

While high catalytic activity is desired in nanozyme applications, specificity is another important factor to be considered, which is essential for achieving selective catalysis, accurate detection, and efficient disease treatment.[192] In recent years, significant efforts have been made to enhance the specificity of nanozymes.[14,105] To optimize the specificity of noble metal-based nanozymes, the enzymatic pathway can be adjusted through substrate binding, substrate conversion, and product release.[192] Recently, $Pd@PtBi_2$ nanospheres were synthesized and exhibited selectively enhanced POD-like activity, enabling the establishment of colorimetric biosensors with high reliability and sensitivity.[14] Additionally, PdSn nanozymes were prepared and showed specific POD-like activity, which could improve the sensitivity and accuracy of the colorimetric immunoassays compared with pure Pd nanozymes.[105] Moreover, Liu *et al.* reported that amine-terminated poly (amidoamine) dendrimer-encapsulated gold nanoclusters could generate O_2 through their intrinsic and specific CAT-like activity, thereby enhancing the efficiency for cancer treatment.[36] It remains highly crucial to further explore more specific nanozymes to meet various application requirements.

4. Biomedical applications of noble metal-based nanozymes

With controllable structure, high activity, and excellent stability, noble metal-based nanozymes have great potential to replace natural enzymes in biomedical applications in the field of biosensing,[26,31] diagnosis,[54] therapeutics,[28,121] and antibacterials.[72,194] In this section, we classified and summarized noble metal-based nanozymes according to their types of applications.

4.1 Sensor

Noble metal-based nanozyme sensors are widely employed for detecting drugs, food processing, and biomolecules because of their high sensitivity, stability, and enzyme-mimicking activity.[195–197] ELISA is a widely used technology for medical diagnostics, in which an enzyme catalyzes a colorimetric reaction, producing a measurable color change (*e.g.*, diamine converted from oxTMB has a characteristic λ_{max} = 450 nm) that reflects the concentration of the target molecule in the sample. Recently, several nanozymes with enhanced POD-like activities have been reported for detecting biomolecules.[18,83,96] For example, Jv *et al.* used Au NPs as POD mimics for colorimetric detection of H_2O_2 [24] and Wu *et al.* used them for glucose detection.[165] In another example, Xi *et al.* compared the LOD of Pd icosahedra and octahedra to illustrate the strain effect on POD-like activities. From the calibration curves of ELISAs to detect carcinoembryonic antigen (CEA, a typical cancer biomarker), the LOD of Pd icosahedra and octahedra were calculated to be 34 pg mL^{-1} and 98 pg mL^{-1}, respectively (Fig. 9a).[82] The LOD of $Ir/WO_{2.72}$ heterostructure for ELISA was 2.2 pg mL^{-1} to CEA, which is 174-fold lower than that of the conventional horseradish peroxidase-based ELISA.[17] In another work, amorphous $RuTe_2$ NRs were synthesized for detecting prostate-specific antigen. A LOD of 32.6 pg ml^{-1} with linear range from 50 pg mL^{-1} to 5 ng mL^{-1} was achieved due to the negligible OxD-like activity, which eliminates the interference of O_2 for colorimetric assays.[95]

Lateral flow immunoassays (LFIAs) have attracted considerable interest in point-of-care testing.[20] Recently, Pd@Pt–Ru-LFIA were fabricated to detect human chorionic gonadotropin.[20] Thanks to the enhanced POD-like activity, with the presence of TMB and H_2O_2, the Pd@Pt–Ru-LFIA exhibited a LOD of 0.1 IU L^{-1} with amplified color responses (Fig. 9b).[20] In addition to hormone detection, Pd@Ir nanocubes were reported as effective nanozymes to detect the gastric cancer biomarkers, pepsinogen I and pepsinogen II.[53] By catalyzing chromogenic substrate deposition, the Pd@Ir NPs were used as a label to produce stronger signals and achieved high sensitivity with a cutoff value as low as 10 pg ml^{-1}.

OxD-like nanozymes can also be used in colorimetric detection, which efficiently transform colorless substrates (*e.g.*, TMB) into colorful products (*e.g.*, TMB^{+}). For example, Pt nanozymes were used to detect isoniazid because the unique pyridine ring of isoniazid inhibited the high OxD-like activity of Pt nanozymes and showed a colorimetric response.[181] Other biosensors based on OxD-like reactions have also been explored for detecting glucose,[186] acetaminophen,[187] *etc*. Additionally, the enzymatic activity can be regulated by surrounding biological substances such as nucleic acid and protein, thus noble metal-based OxD-like nanozymes have also shown potential in detecting a wider library of substances like cytokine interleukin 2 [29] and DNA hybridization.[198]

4.2 Antibiosis

Pathogenic infections caused by bacterial, viral, and fungal pathogens pose major global health challenges, further aggravated by the rise of antimicrobial resistance and the growing scarcity of effective antibiotics.[199] Recently, noble metal-based nanozymes have emerged as promising alternatives for com-

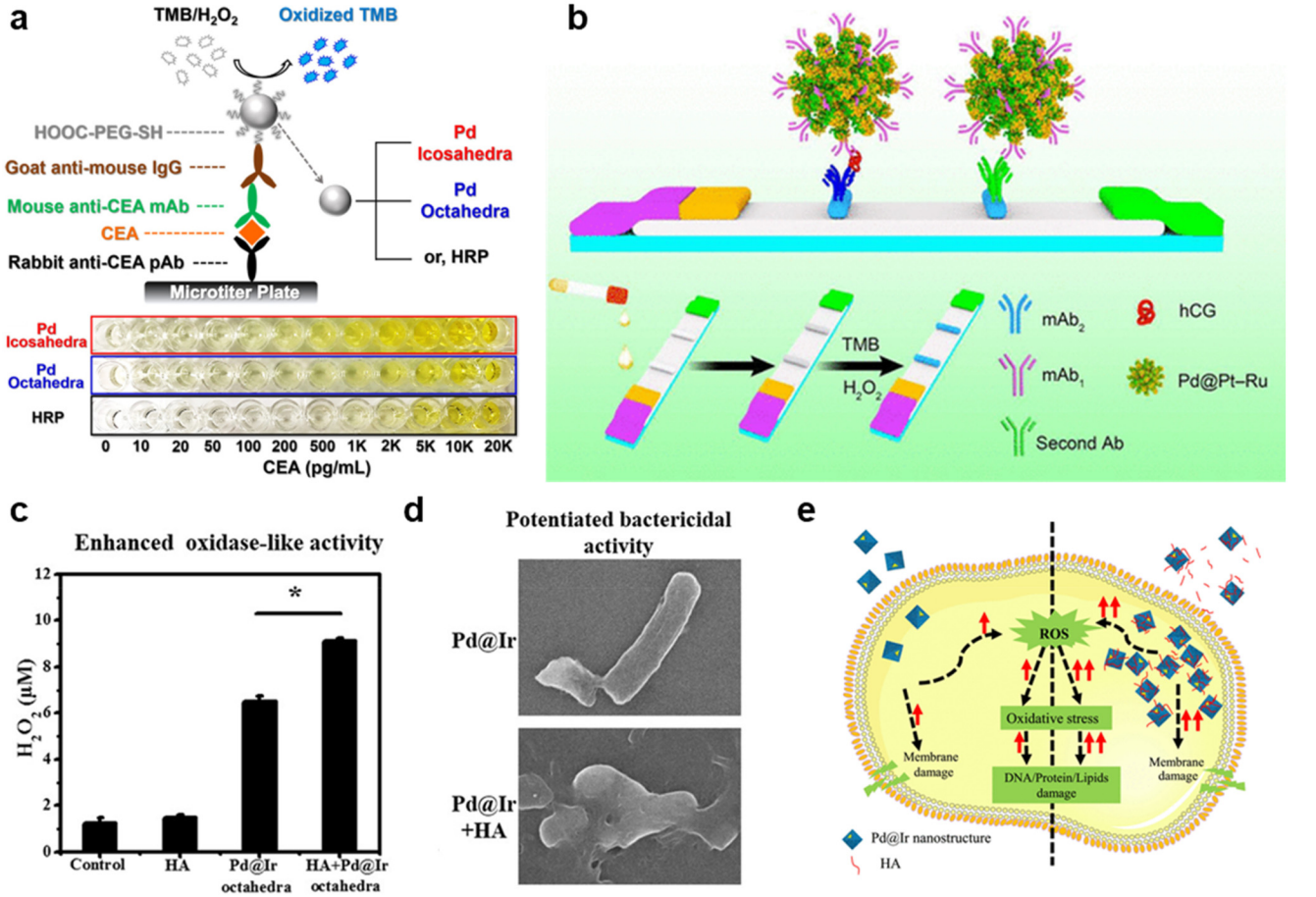

Fig. 9 (a) Scheme of the colorimetric enzyme-linked immunosorbent assay (ELISA) of carcinoembryonic antigen (CEA) and photographs showing the different detection sensitivity Pd icosahedra-ELISA (top), Pd octahedra-ELISA (middle), and HRP-ELISA (bottom) using standard CEA concentrations. The yellow-colored product comes from the oxidized TMB. Reproduced with permission from ref. 80. Copyright 2019, American Chemical Society. (b) Schematic diagram of lateral flow immunoassays (LFIA) application of Pd@Pt–Ru NPs. Antibody and Pd@Pt–Ru NPs were conjugated and assembled into a LFIA for human chorionic gonadotropin detection. Reproduced with permission from ref. 20. Copyright 2024, American Chemical Society (c) Comparison of OxD-like activities with and without the addition Pd@Ir nanostructures and humic acid (HA). A significant increase in the H_2O_2 concentration was observed with Pd@Ir nanostructures and HA, indicating HA could enhance the OxD-like activity of Pd@Ir nanostructures. (d) Typical SEM images of bacterial cells after different treatments, showing more severe damage to the bacterial membrane in the presence of HA. (e) Possible mechanisms for the potentiated antibacterial activity of Pd@Ir nanostructures in the presence of HA. Reproduced with permission from ref. 194. Copyright 2019, American Chemical Society.

bating bacterial infections due to their ability to mimic OxD and POD activities for ROS generation or oxidative modulation.[199] For instance, the antibacterial ability of OxD-mimic Pd@Ir octahedra against *Escherichia coli*, *Staphylococcus aureus*, *Bacillus subtilis* and *Salmonella enteritidis* has been verified.[194] The bactericidal activity of Pd@Ir octahedra was significantly enhanced in the presence of humic acid, leading to elevated levels of ROS. The ROS induced oxidative damage to essential biomacromolecules, including DNA, proteins, and lipids, effectively contributing to bacterial eradication (Fig. 9c–e).[194] Similarly, by generating high-level ROS, mesoporous silica-supported AuNPs possessing dual enzyme activities (POD-like and OxD-like activities) were prepared to kill the pathogenic bacteria.[200] Additionally, an antibacterial agent was developed *via* doping Ag into oxygen-vacancy-enriched glucose-modified MoO_x.[185] The resultant nanozyme heterostructure exhibited NIR-enhanced OxD-like activity, which helped to generate ROS and greatly enhanced antimicrobial activities against multidrug-resistant bacteria.[185]

4.3 Disease treatment

With their intrinsic antioxidant or pro-oxidant activity, noble metal-based nanozymes are also widely used in disease treatment. Nanozymes with antioxidant activities, like CAT and SOD mimics, regulate ROS to treat diseases related to oxidative stress, while pro-oxidant nanozymes, such as OxD and POD mimics, generate ROS *in vivo*, enabling applications in anticancer, anti-inflammatory, *etc.*[60] For example, PtMo-Au nanozyme with CAT-like activity was developed for tumor therapy by continuously catalyzing the decomposition of H_2O_2 to O_2.[8] Apart from tumor therapy, anti-oxidant activities are also used to protect cells and tissues by decreasing ROS and relieving

oxidative stress. For instance, by scavenging UV-induced cellular ROS, surface-functionalized Au–Pt NCs nanozymes protected cells *in vivo* from the UV-induced oxidative stress damage.[201] Ming *et al.* designed and fabricated a Pd–Ru/uricase@red blood cell nanoreactor that could efficiently degrade H_2O_2 through its CAT-like activity,[189] facilitating uricase oxidation and enabling the safe and effective treatment of hyperuricemia with minimal side effects. In a study model of lipopolysaccharide-induced brain injury, the SOD-like activity of PdPtMo nanozymes helped to treat the lipid peroxidation, with increased survival rate of injured mice. With their ability in regulating ROS, nanozymes with antioxidant activities are also applied in H_2O_2-associated inflammation.[202] Chen *et al.* synthesized a CeO_2/Pt nanozyme in cross-linked zwitterionic vesicles, which could resist protein adsorption efficiently and hold a good therapeutic effect in ROS-induced ear inflammation.[142] In addition to therapeutic function, Pt-based nanozyme heterostructures, like the Pt@PCN222-Mn with SOD- and CAT-like activities, were also used for anti-inflammatory therapy, which could effectively relieve two forms of inflammatory bowel disease, ulcerative colitis and Crohn's disease, by catalyzing the anti-ROS cascade reaction *in vivo*.[155] In another example, bovine serum albumin-coated RuO_2 NPs were reported as SOD- and CAT-like nanozymes to transform $O_2^{\bullet-}$ into H_2O_2 and subsequently decompose H_2O_2 into oxygen, which remarkably reduced the infarcted area and restored cardiac function in ischemic myocardium.[203]

Different from antioxidant nanozymes, pro-oxidant nanozymes play a role by generating a large amount of ROS for disease treatment. For example, biocompatible Zr-based MOFs with an Ir-porphyrin linker exhibited remarkable stability, strong H_2O_2 adsorption energy, and high POD-like catalytic activity, inducing abundant ROS for an effective antitumor effect.[204] In another work, Jia *et al.* reported an AgPd bimetallic nanozyme with significantly enhanced POD-like activity which efficiently decomposed H_2O_2 to generate a large number of $^{\bullet}OH$ in an acidic environment for ROS-killing-tumor therapy.[67]

Apart from the excellent enzyme-like activities of noble metal-based nanozymes, their unique physicochemical properties can also be integrated for multifunctional disease treatment. For instance, noble metal-based nanozymes can convert

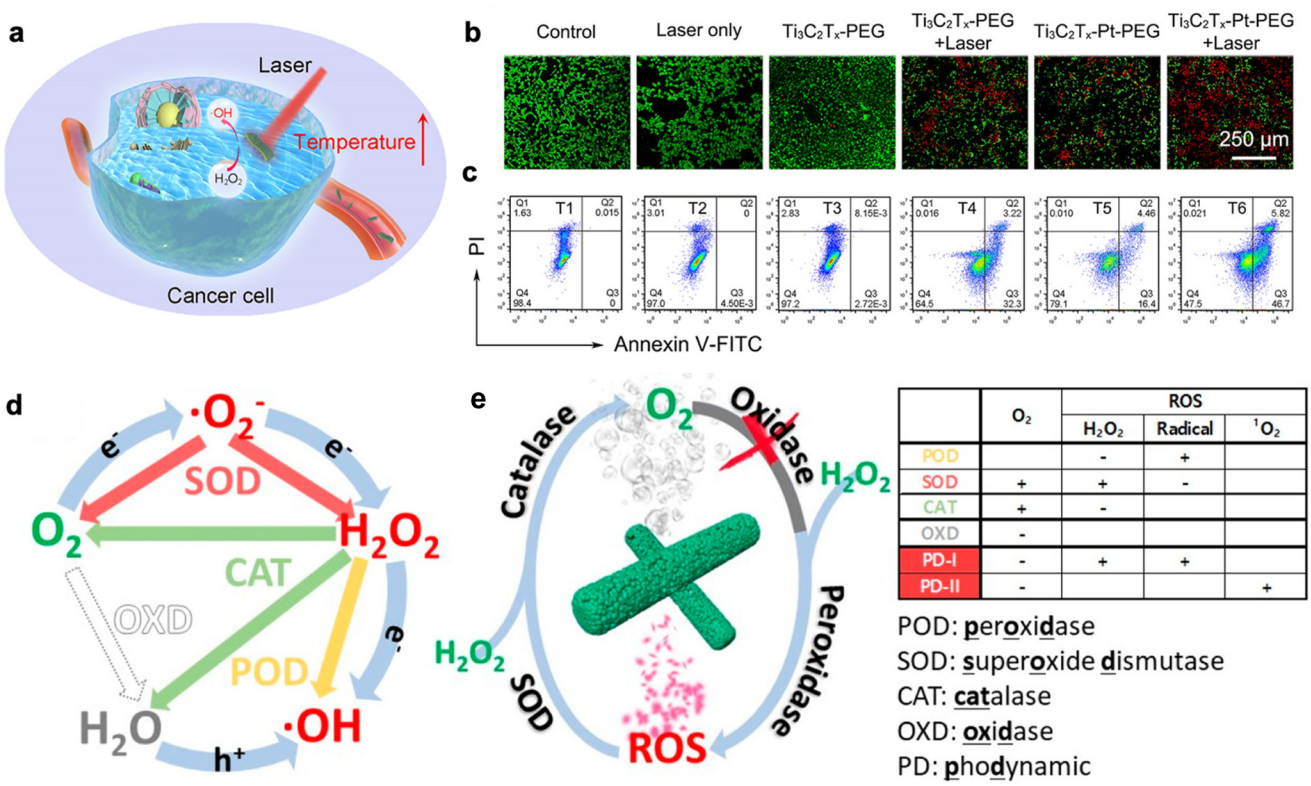

	O_2	ROS		
		H_2O_2	Radical	$^1O_2$
POD		-	+	
SOD	+	+	-	
CAT	+	-		
OXD	-			
PD-I	-	+	+	
PD-II	-			+

Fig. 10 (a) Schematic illustration of photothermal-enhanced enzymatic catalytic activities for cancer treatment using $Ti_3C_2T_x$-Pt-PEG nanocomposites, where the temperature increase significantly enhances the POD-like activity. (b) The calcein acetoxymethyl ester (green) and propidium iodide (red) double-staining assay and (c) flow cytometry analysis of 4T1 cells incubated with different treatments (T1: control group without any treatment; T2: laser only; T3: $Ti_3C_2T_x$-PEG nanocomposites; T4: $Ti_3C_2T_x$-PEG nanocomposites + laser; T5: $Ti_3C_2T_x$-Pt-PEG nanocomposites; T6: $Ti_3C_2T_x$-Pt-PEG nanocomposites + laser). Reproduced with permission from ref. 141, Copyright 2022, American Chemical Society. (d) Schematic illustration showing the synergistic SOD-, CAT-, and POD-like enzymatic cycle (indicated by straight arrows) and the photocatalytic cycle (indicated by curved arrows) for cancer treatment. (e) Schematic illustration showing how the simultaneous SOD-, CAT-, and POD-like enzymatic activities of Ru–Te nanorods generate O_2 and ROS to overcome hypoxia in photodynamic therapy. The table records the positive and negative feedback of O_2 or ROS in different enzymatic and photodynamic processes. Reproduced with permission from ref. 206, Copyright 2020, American Chemical Society.

captured light energy into thermal energy, thereby increasing temperature and acting as PTT agents for synergistic treatment.[205] Zhu *et al*. synthesized $Ti_3C_2T_x$-Pt-PEG nanocomposites, which exhibited a significant temperature increase to 48.1 °C within 5 minutes under irradiation with NIR-II light at 1064 nm. The high photothermal conversion efficiency (η = 31.78%) and stability of $Ti_3C_2T_x$-Pt-PEG nanocomposites ensure their potential in killing cancer cells.[141] As expected, the POD-like activities were enhanced with temperature, generating more highly toxic $^{\bullet}OH$ to kill breast cancer cells (Fig. 10a). *In vitro* experiments confirmed their efficacy in phototheragnostics, demonstrating synergistic ablation of cancer cells (Fig. 10b and c). In another similar work, OxD-like activities of RhRu nanozymes were enhanced upon exposure to a 1064 nm laser that resulted in a temperature increase. The OxD-like activities were found to be 1.33-fold higher than those of counterparts without irradiation. Additionally, noble metal-based nanozymes have been reported as photosensitizers for PDT. During the PDT process, non-toxic photosensitizers are activated by irradiation to generate ROS, such as $^{\bullet}OH$ (type I PDT against hypoxia) and $^1O_2$ (type II PDT against hypoxia). For instance, a Ru–Te nanorod-based enzymatic platform showed a synergistic effect of PDT and enzymatic treatment, showing high efficiency in hypoxic pancreatic cancer phototherapy both *in vitro* and *in vivo*. The O_2 produced by the CAT-like Ru–Te NRs could promote the generation of $^1O_2$ *via* the type II photodynamic reaction, while the POD- and SOD-like reactions of Ru–Te NRs helped overcome the rapid quenching of $^{\bullet}OH$ and H_2O_2 species generated from the type I photodynamic process under hypoxic conditions (Fig. 10d).[206] Similar to PDT, sonodynamic therapy (SDT) is also a promising non-invasive therapeutic modality, based on sonosensitizers activated by low-intensity ultrasound to produce ROS for cancer therapy. Recently, $PtCu_3$ nanocages were synthesized and utilized as sonosensitizers to generate ROS, including $^{\bullet}OH$ and $^1O_2$.[47] *In vitro* and *in vivo* studies of $PtCu_3$ nanocages confirmed their ability to generate ROS under ultrasound irradiation, which effectively delayed the tumor growth.[47] In another work, multifunctional nanozymes composed of Au NPs, carbon dots, and TiO_2 hollow nanospheres showed multiple enzyme-like activities and ultrasonic response, which could form sufficient oxygen to alleviate the hypoxia condition in the tumor microenvironment and generate abundant ROS.[207]

Immunotherapy is a unique treatment methodology that fights disease by activating or suppressing the patient's immune system. For example, cGAS-STING, short for cyclic guanosine monophosphate (GMP)-adenosine monophosphate (AMP) synthase (cGAS)-stimulator of interferon genes, has been identified as an innate immune signaling pathway to induce interferon production and therapeutic effects.[18] Li *et al.* found that the Mn^{2+} in immune-responsive PtMnIr nanozymes could activate the cGAS-STING pathway with increased expression of interferons, which helped to prevent tumor metastasis.[18] In addition, AuPtAg-GOx nanozymes were developed for synergistic tumor immunotherapy, demonstrating their potential in cancer treatment.[208] Furthermore, PdPtCu trimetallic nanozymes were reported to trigger immunogenic cell death and activate the antitumor immune response, highlighting the role they can play in advancing immunotherapeutic strategies.[11]

5. Conclusion and perspective

In this review, we systematically summarize recent progress in the field of noble metal-based nanozymes, focusing on their structural regulations and biomedical applications. As structural factors are closely correlated with the exposed surface atoms and active sites, a broad spectrum of examples are used to illustrate that the enzyme-like activities of noble metal-based nanozymes can be tuned by size, morphologies, strain, crystallinity, alloying, ligand, and chemical compositions. Furthermore, the roles of noble metal-based nanozymes as catalysts are discussed for enzyme-like reactions including POD, CAT, OxD, SOD, and so on. Synergistic catalysis involving multi-enzyme mimics as well as highly specific selective catalysis are also critical for enzyme mimics in advanced biomedical applications. Consequently, noble metal-based nanozymes have shown great potential to replace natural enzymes in sensors, antibiosis, and disease treatment. Several multimodal treatments utilizing unique physicochemical properties of noble metal-based nanozymes, including PTT, PDT, and SDT, are also discussed. Despite remarkable progress in this area, many challenges and opportunities are present in the further development of noble metal-based nanozymes.

5.1 Fine structural design of noble metal-based nanozymes

While significant advancements in structural control of noble metal nanomaterials have been made over the past decade, precisely controlled nanostructures with specific facets, crystallinity, and components remain limited in the field of nanozymes. For example, noble metal-based nanomaterials with tailorable atomic arrangements, including intermetallic compounds and unconventional-phase metals, have rarely been applied as nanozymes. Currently, there is insufficient fundamental research focusing on the design and synthesis of fine noble metal-based nanocrystals towards enhanced enzymatic activity, stability, and/or dispersity. More efforts are desired to develop novel noble metal-based nanozymes and to gain deeper insights into their rational structural design towards specific nanozyme applications. Thanks to the development of computational technology, artificial intelligence (AI) may further assist in novel nanozyme prediction, design and performance optimization. Through AI-driven design and experimental validation, we can further accelerate the creation and optimization of nanozyme structures to greatly widen the nanozyme library.

5.2 Structure–"enzyme-like property"–performance relationships

Although some investigations have been made into the structural effects on enzymatic performances of noble metal-based

nanozymes, the interpretation of the structure–performance relationship is generally vague, and sometimes even contradictory. For example, alloying Au into Ag(111) facet has been reported to enhance OxD-like activities, whereas the opposite effect occurs when alloying Au into Pd(111) facets.[74] The enzyme-like properties, such as binding strength of substrates, electron transfer, and product release, lack specific investigation. Therefore, experimental designs to systematically investigate the structure–"enzyme-like property"–performance relationships are crucial for the development of noble metal-based nanozymes. Besides, the exploration of enzymatic performance primarily focuses on POD- and OxD-like activities, while research on the other types of enzyme activity is relatively limited.

Meanwhile, the commonly existing multiple enzyme-like activities and specificity in nanozymes have become key issues in disease diagnosis and treatment. To take full advantage of the self-cascade synergistic catalysis, the synergy between different enzymatic activities must be sorted out and correlated to specific structural factors of a nanozyme. Additionally, research on specificity of noble metal-based nanozymes is still in the early stage and needs more in-depth research focus.

5.3 In-depth catalytic mechanisms study

Despite considerable efforts, studies on the working mechanisms of noble metal-based nanozymes are still limited to specific microenvironments and idealized conditions, making theoretical results deviate from experimental ones. Additionally, limitations in characterization techniques make it challenging to obtain direct experimental evidence to verify the key catalytic sites of nanozymes, the dynamic changes during the catalytic process, or the critical intermediates. An integration of high-throughput experiments, theoretical calculations, and advanced characterizations (*e.g.*, *in situ* characterizations) will provide deeper mechanistic insights in various biochemical reactions.

5.4 Exploration of multifunctional nanozymes

Noble metal-based nanozymes integrate their unique physicochemical properties with enzyme-like activity, endowing them with multiple functionalities. Further expanding the functionalities of noble metal-based nanozymes by introducing more functional components could be a promising research direction. For example, noble metal nanozymes can be easily magnetically recycled by introducing magnetic components, or can act as SDT agents when combined with sonosensitizers. Future exploration of noble metal-based nanozymes with expanded functionalities could enable innovative applications in more practical scenarios.

5.5 Biosafety

The biosafety of nanozymes has been a critical issue in biomedical applications. Although noble metal-based nanozymes have shown great potential in antioxidation, antibiosis, disease treatment, biosensing, and bioimaging, their biosafety, which may be affected by various factors such as concentration, temperature, and pH value, remains a significant concern. While some structural regulation strategies (*e.g.*, reducing size and surface modification) have been developed to mitigate the toxicity of noble metal based-nanozymes, their biosafety in practical applications has not been comprehensively assessed.

5.6 Towards practical applications

Although various noble metal-based nanozymes have been reported with significant potential in biomedical applications, further breakthroughs are essential towards their practical applications. Firstly, large-scale, commercial synthesis of these nanozymes has not yet been achieved, and their structural control is often sensitive to reaction conditions, limiting the conversion of products from laboratory to industry. Secondly, while a diverse range of noble metal-based nanozymes have been reported, there is a lack of a comprehensive database covering their key information, such as cost, synthetic methods, and functionality. AI-based machine learning holds great potential for information integration in this field. By using AI-assisted technology, we can establish a database that includes the classification, fabrication, and performance evaluation of nanozymes, including noble metals and others. The database would be beneficial for academic research and large-scale production of nanozymes. Finally, to facilitate the widespread application of noble metal-based nanozymes, it is crucial to develop a standardized evaluation system that quantitatively assesses key parameters of nanozymes such as morphology, dispersibility, stability, enzyme-like activity, and biosafety.

In summary, we believe that noble metal-based nanozymes possess great potential for biomedical applications, relying not only on their inherently catalytic activity but also on their unique physicochemical properties. Structural regulation is an effective method for modulating enzyme-like activity, specificity, and multifunctionality in noble metal-based nanozymes. Despite the challenges and obstacles, future development of noble metal-based nanozymes is expected to address these issues and unlock new possibilities in biomedical applications and beyond.

Data availability

No primary research results, software or code have been included and no new data were generated or analysed as part of this review.

Conflicts of interest

There are no conflicts to declare.

Acknowledgements

Y. C. is grateful for the funding support from the NSFC Young Scientists Fund (project no. 22305203), the support from the

Start-up Fund (project no. 4930977) from The Chinese University of Hong Kong, and the support from the Hong Kong Branch of the National Precious Metals Material Engineering Research Center (NPMM) at City University of Hong Kong.

References

1 X. T. Ding, Z. Zhao, Y. F. Zhang, M. L. Duan, C. Z. Liu and Y. H. Xu, *Small*, 2023, **19**, 2207142.
2 M. Wittwer, U. Markel, J. Schiffels, J. Okuda, D. F. Sauer and U. Schwaneberg, *Nat. Catal.*, 2021, **4**, 814–827.
3 R. F. Zhang, X. Y. Yan and K. L. Fan, *Acc. Mater. Res.*, 2021, **2**, 534–547.
4 Y. Y. Huang, J. S. Ren and X. G. Qu, *Chem. Rev.*, 2019, **119**, 4357–4412.
5 J. J. X. Wu, S. R. Li and H. Wei, *Nanoscale Horiz.*, 2018, **3**, 367–382.
6 L. Li, Y. Hu, Y. Shi, Y. Liu, T. Liu, H. Zhou, W. Niu, L. Zhang, J. Zhang and G. Xu, *Chem. Eng. J.*, 2023, **463**, 142494.
7 M. W. Ji, M. Xu, W. Zhang, Z. Z. Yang, L. Huang, J. J. Liu, Y. Zhang, L. Gu, Y. X. Yu, W. C. Hao, P. F. An, L. R. Zheng, H. S. Zhu and J. T. Zhang, *Adv. Mater.*, 2016, **28**, 3094–3101.
8 M. J. Chao, S. M. Tai, M. X. Mao, W. B. Cao, C. F. Peng, W. Ma, Y. W. Feng and Z. P. Wang, *Aggregate*, 2025, **6**, e644.
9 F. Wei, X. Y. Cui, Z. Wang, C. C. Dong, J. D. Li and X. J. Han, *Chem. Eng. J.*, 2021, **408**, 127240.
10 Y. Y. Zhao, J. Yang, G. Y. Shan, Z. Y. Liu, A. Cui, A. L. Wang, Y. W. Chen and Y. C. Liu, *Sens. Actuators, B*, 2020, **305**, 127420.
11 Y. L. Xie, M. Wang, Y. R. Qian, L. Li, Q. Q. Sun, M. H. Gao and C. X. Li, *Small*, 2023, **19**, 2303596.
12 G. Q. Song, X. Y. Shao, C. Qu, D. H. Shi, R. Jia, Y. F. Chen, J. P. Wang and H. L. An, *Chem. Eng. J.*, 2023, **477**, 147161.
13 Y. J. Tang, Y. J. Chen, Y. Wu, W. Q. Xu, Z. Luo, H. R. Ye, W. L. Gu, W. Y. Song, C. Z. Zhu and S. J. Guo, *Nano Lett.*, 2023, **23**, 267–275.
14 M. D. Lei, X. L. Ding, J. Liu, Y. J. Tang, H. X. Chen, Y. Zhou, C. Z. Zhu and H. Y. Yan, *Anal. Chem.*, 2024, **96**, 6072–6078.
15 Z. Xi, W. W. Gao and X. H. Xia, *ChemBioChem*, 2020, **21**, 2440–2444.
16 S. S. Li, B. L. Xu, H. K. Yang, C. Zhang, J. L. Chen, S. Liu, Z. J. Huang and H. Y. Liu, *Small*, 2024, **20**, 2309704.
17 Z. Xi, W. W. Gao, A. Biby, A. Floyd and X. H. Xia, *ACS Appl. Nano Mater.*, 2022, **5**, 6089–6093.
18 D. Y. Li, E. Ha, Z. L. Zhou, J. G. Zhang, Y. Y. Zhu, F. J. Ai, L. Yan, S. Q. He, L. Li and J. Q. Hu, *Adv. Mater.*, 2024, **36**, 2308747.
19 J. Yang, L. Fang, R. B. Jiang, L. B. Qi, Y. T. Xiao, W. X. Wang, I. Ismail and X. H. Fang, *Adv. Healthcare Mater.*, 2023, **12**, 2300490.
20 W. G. Wang, Q. Q. Cao, J. He, Y. F. Xie, Y. Zhang, L. Yang, M. H. Duan, J. K. Wang and W. Li, *Nano Lett.*, 2024, **24**, 8311–8319.
21 J. P. Wang, J. Y. Sun, W. Hu, Y. H. Wang, T. M. Chou, B. L. Zhang, Q. Zhang, L. Ren and H. J. Wang, *Adv. Mater.*, 2020, **32**, 2001862.
22 C. Yang and L. F. Cui, *Green Energy Environ.*, 2023, **8**, 1–3.
23 C. S. Shang, Q. Q. Wang, H. Tan, S. Y. Lu, S. G. Wang, Q. H. Zhang, L. Gu, J. Li, E. R. Wang and S. J. Guo, *JACS Au*, 2022, **2**, 2453–2459.
24 Y. Jv, B. X. Li and R. Cao, *Chem. Commun.*, 2010, **46**, 8017–8019.
25 D. T. Xu, L. Y. Wu, H. D. Yao and L. N. Zhao, *Small*, 2022, **18**, 2203400.
26 Z. F. Wang, Y. Yan, C. Li, Y. Yu, S. Cheng, S. Chen, X. J. Zhu, L. P. Sun, W. Tao, J. W. Liu and F. Wang, *ACS Nano*, 2022, **16**, 9019–9030.
27 Y. M. Sun, S. D. Mu, Z. Y. Xing, J. S. Guo, Z. H. Wu, F. Y. Yu, M. R. Bai, X. L. Han, C. Cheng and L. Ye, *Adv. Mater.*, 2022, **34**, 2206208.
28 Y. Wu, W. Q. Xu, L. Jiao, Y. J. Tang, Y. F. Chen, W. L. Gu and C. Z. Zhu, *Mater. Today*, 2022, **52**, 327–347.
29 W. W. He, Y. Liu, J. S. Yuan, J. J. Yin, X. C. Wu, X. N. Hu, K. Zhang, J. B. Liu, C. Y. Chen, Y. L. Ji and Y. T. Guo, *Biomaterials*, 2011, **32**, 1139–1147.
30 J. Lee, M. H. Kim, H. Lee, J. Kim, J. Seo, H. W. Lee, C. Hwang and H. K. Song, *Angew. Chem., Int. Ed.*, 2023, **62**, e202312928.
31 H. Q. Zhao, R. F. Zhang, X. Y. Yan and K. L. Fan, *J. Mater. Chem. B*, 2021, **9**, 6939–6957.
32 G. P. Xu, X. C. Du, W. J. Wang, Y. Y. Qu, X. D. Liu, M. W. Zhao, W. F. Li and Y. Q. Li, *Small*, 2022, **18**, 2204131.
33 N. A. Bakar, N. N. Yusoff, F. S. N. Azmi and J. G. Shapter, *Aggregate*, 2023, **4**, e339.
34 S. Fiorito, N. Soni, N. Silvestri, R. Brescia, H. GavilOn, J. S. Conteh, B. T. Mai and T. Pellegrino, *Small*, 2022, **18**, 2200174.
35 J. D. Wu, Q. H. Liu, D. X. Jiao, B. Tian, Q. Wu, X. Chang, H. Y. Chu, S. Jiang, Q. Yang, T. Liu, Y. Zhang, W. Zhang, J. C. Fan, X. Q. Cui and F. F. Chen, *Angew. Chem., Int. Ed.*, 2024, **63**, e202403203.
36 C. P. Liu, T. H. Wu, C. Y. Liu, K. C. Chen, Y. X. Chen, G. S. Chen and S. Y. Lin, *Small*, 2017, **13**, 1700278.
37 C. Y. Cao, H. Zou, N. Yang, H. Li, Y. Cai, X. J. Song, J. J. Shao, P. Chen, X. Z. Mou, W. J. Wang and X. C. Dong, *Adv. Mater.*, 2021, **33**, 2106996.
38 Z. Q. Lv, S. J. He, Y. F. Wang and X. Y. Zhu, *Adv. Healthcare Mater.*, 2021, **10**, 2001806.
39 X. Y. Cui, M. H. Li, L. Tong, M. J. Li, X. F. Tang and X. J. Han, *Colloids Surf., B*, 2023, **223**, 113168.
40 Y. M. Ju, H. L. Zhang, J. Yu, S. Y. Tong, N. Tian, Z. Y. Wang, X. B. Wang, X. T. Su, X. Chu, J. Lin, Y. Ding, G. J. Li, F. G. Sheng and Y. L. Hou, *ACS Nano*, 2017, **11**, 9239–9248.
41 Y. Yang, M. Chen, B. Z. Wang, P. Wang, Y. C. Liu, Y. Zhao, K. Li, G. S. Song, X. B. Zhang and W. H. Tan, *Angew. Chem., Int. Ed.*, 2019, **58**, 15069–15075.

42 W. Duan, J. L. Wang, X. M. Peng, S. F. Cao, J. J. Shang, Z. W. Qiu, X. Q. Lu and J. B. Zeng, *Biosens. Bioelectron.*, 2023, **223**, 115022.
43 Y. Huang, Y. Q. Gu, X. Y. Liu, T. T. Deng, S. Dai, J. F. Qu, G. H. Yang and L. L. Qu, *Biosens. Bioelectron.*, 2022, **209**, 114253.
44 M. Xu, X. Zhang, B. W. Dong, W. J. Wang and Z. H. Zhao, *Part. Part. Syst. Charact.*, 2023, **41**, 2300135.
45 L. Ding, Y. Chen, B. Zhang, R. Z. Hu, C. Dai, C. H. Dong and H. Huang, *ACS Nano*, 2022, **16**, 15959–15976.
46 X. Meng, H. Fan, L. Chen, J. He, C. Hong, J. Xie, Y. Hou, K. Wang, X. Gao, L. Gao, X. Yan and K. Fan, *Nat. Commun.*, 2024, **15**, 1626.
47 X. Y. Zhong, X. W. Wang, L. Cheng, Y. A. Tang, G. T. Zhan, F. Gong, R. Zhang, J. Hu, Z. Liu and X. L. Yang, *Adv. Funct. Mater.*, 2020, **30**, 1907954.
48 F. Xia, X. Hu, B. Zhang, X. Wang, Y. A. Guan, P. H. Lin, Z. Y. Ma, J. P. Sheng, D. S. Ling and F. Y. Li, *Small*, 2022, **18**, 2201558.
49 Y. Chong, X. Dai, G. Fang, R. F. Wu, L. Zhao, X. C. Ma, X. Tian, S. Y. Lee, C. Zhang, C. Y. Chen, Z. F. Chai, C. C. Ge and R. H. Zhou, *Nat. Commun.*, 2018, **9**, 4861.
50 S. Yougbare, H. L. Chou, C. H. Yang, D. I. Krisnawati, A. Jazidie, M. Nuh and T. R. Kuo, *J. Hazard. Mater.*, 2021, **407**, 124617.
51 H. Z. Fan, J. J. Zheng, J. Y. Xie, J. W. Liu, X. F. Gao, X. Y. Yan, K. L. Fan and L. Z. Gao, *Adv. Mater.*, 2023, **36**, 2300387.
52 Z. Xi, K. C. Wei, Q. X. Wang, M. J. Kim, S. H. Sun, V. Fung and X. H. Xia, *J. Am. Chem. Soc.*, 2021, **143**, 2660–2664.
53 X. M. Meng, W. C. Zuo, P. C. Wu, Y. H. Song, G. J. Yang, S. B. Zhang, J. Yang, X. P. Zou, W. L. Wei, D. H. Zhang, J. J. Dai and Y. M. Ju, *Nano Lett.*, 2023, **24**, 51–60.
54 S. H. Tang, M. Chen and N. F. Zheng, *Small*, 2014, **10**, 3139–3144.
55 D. Wen, K. Li, R. P. Deng, J. Feng and H. J. Zhang, *J. Am. Chem. Soc.*, 2023, **145**, 3952–3960.
56 Y. Y. Li, Z. H. Zeng, J. J. Tong, T. Yang, G. H. Liu, B. Feng, P. Zhang, X. F. Liu and T. P. Qing, *Appl. Surf. Sci.*, 2024, **655**, 159695.
57 S. S. Li, B. L. Xu, M. Z. Lu, M. X. Sun, H. K. Yang, S. Liu, Z. J. Huang and H. Y. Liu, *Adv. Mater.*, 2022, **34**, 2202609.
58 Y. F. Shi, Z. H. Lyu, M. Zhao, R. H. Chen, Q. N. Nguyen and Y. N. Xia, *Chem. Rev.*, 2021, **121**, 649–735.
59 H. L. Liu, F. Nosheen and X. Wang, *Chem. Soc. Rev.*, 2015, **44**, 3056–3078.
60 L. Su, S. N. Qin, Z. J. Xie, L. Wang, K. Khan, A. K. Tareen, D. F. Li and H. Zhang, *Coord. Chem. Rev.*, 2022, **473**, 214784.
61 C. Ma, W. W. Chen, Y. J. Wu, W. B. Wang, L. Xu, C. S. Chen, L. Zheng, G. Wang, P. Han, P. Gu, X. Wang, Y. Zhu, Z. Y. Zeng, H. Y. He, Q. Y. He, Z. H. Ke, D. Su and Y. Chen, *Nano Lett.*, 2025, **25**, 3212–3220.
62 R. F. Wu, Y. Chong, G. Fang, X. M. Jiang, Y. Pan, C. Y. Chen, J. J. Yin and C. C. Ge, *Adv. Funct. Mater.*, 2018, **28**, 1801484.
63 G. T. Yuan, S. T. Zhang, Z. X. Yang, S. J. Wu, H. J. Chen, X. Tian, S. Cheng, Y. Pan and R. H. Zhou, *Biomater. Sci.*, 2022, **10**, 7067–7076.
64 Y. N. Liu, D. L. Huo, X. F. Zhu, X. Chen, A. G. Lin, Z. Jia and J. Liu, *Nanoscale*, 2021, **13**, 14900–14914.
65 H. F. Zhang, J. Tan, X. Q. Yang, Y. Y. Ma, H. Y. Zou, Y. Wang, P. Zhang and Y. Q. Zheng, *ACS Appl. Nano Mater.*, 2022, **5**, 10818–10828.
66 H. H. Ye, J. Mohar, Q. X. Wang, M. Catalano, M. J. Kim and X. H. Xia, *Sci. Bull.*, 2016, **61**, 1739–1745.
67 T. Jia, D. Li, J. R. Du, X. K. Fang, V. Gerasimov, H. Ågren and G. Y. Chen, *J. Nanobiotechnol.*, 2022, **20**, 424.
68 X. Wang, S. J. Chen, X. M. Tang, D. Q. Lin and P. Qiu, *RSC Adv.*, 2019, **9**, 36578–36585.
69 R. T. P. da Silva, M. P. D. Rodrigues, G. F. B. Davilla, A. M. R. P. da Silva, A. H. B. Dourado and S. I. C. de Torresi, *ACS Appl. Nano Mater.*, 2021, **4**, 12062–12072.
70 Z. Xi, J. Xie, J. Hu, Q. C. Wang, Z. Y. Wang, X. Q. Yang, L. Y. Zong, M. Y. Zhang, X. H. Sun, S. H. Sun and J. Han, *Nano Lett.*, 2024, **24**, 3432–3440.
71 S. Y. Xu, X. J. Dong, S. Q. Chen, Y. Y. Zhao, G. Y. Shan, Y. C. Sun, Y. W. Chen and Y. C. Liu, *Sens. Actuators, B*, 2019, **281**, 375–382.
72 G. Fang, W. F. Li, X. M. Shen, J. M. Perez-Aguilar, Y. Chong, X. F. Gao, Z. F. Chai, C. Y. Chen, C. C. Ge and R. H. Zhou, *Nat. Commun.*, 2018, **9**, 129.
73 S. S. Li, K. Gu, H. Wang, B. L. Xu, H. W. Li, X. H. Shi, Z. J. Huang and H. Y. Liu, *J. Am. Chem. Soc.*, 2020, **142**, 5649–5656.
74 X. M. Shen, W. Q. Liu, X. J. Gao, Z. H. Lu, X. C. Wu and X. F. Gao, *J. Am. Chem. Soc.*, 2015, **137**, 15882–15891.
75 J. S. Zhang, Y. N. Liu, L. S. Cui, S. J. Hao, D. Q. Jiang, K. Y. Yu, S. C. Mao, Y. Ren and H. Yang, *Adv. Mater.*, 2020, **32**, 1904387.
76 D. B. Kim, J. Y. Kim, J. Han and Y. S. Cho, *Nano Energy*, 2024, **125**, 109551.
77 X. B. Yang, Y. Y. Wang, X. L. Tong and N. J. Yang, *Adv. Energy Mater.*, 2022, **12**, 2102261.
78 L. Wang, Z. H. Zeng, W. P. Gao, T. Maxson, D. Raciti, M. Giroux, X. Q. Pan, C. Wang and J. Greeley, *Science*, 2019, **363**, 870–874.
79 H. Chen, B. Zhang, X. Liang and X. X. Zou, *Chin. J. Catal.*, 2022, **43**, 611–635.
80 G. G. Liu, W. Zhou, Y. R. Ji, B. Chen, G. T. Fu, Q. B. Yun, S. M. Chen, Y. X. Lin, P. F. Yin, X. Y. Cui, J. W. Liu, F. Q. Meng, Q. H. Zhang, L. Song, L. Gu and H. Zhang, *J. Am. Chem. Soc.*, 2021, **143**, 11262–11270.
81 C. R. Kao, A. H. Yeh, B. H. Chen, L. M. Lyu, Y. C. Chuang, B. T. Sneed and C. H. Kuo, *Chem. Mater.*, 2022, **34**, 2282–2291.
82 Z. Xi, X. Cheng, Z. Q. Gao, M. J. Wang, T. Cai, M. Muzzio, E. Davidson, O. Chen, Y. Jung, S. H. Sun, Y. Xu and X. H. Xia, *Nano Lett.*, 2020, **20**, 272–277.
83 X. H. Xia, J. T. Zhang, N. Lu, M. J. Kim, K. Ghale, Y. Xu, E. McKenzie, J. B. Liu and H. H. Yet, *ACS Nano*, 2015, **9**, 9994–10004.

84 Y. Chen, Z. C. Lai, X. Zhang, Z. X. Fan, Q. Y. He, C. L. Tan and H. Zhang, *Nat. Rev. Chem.*, 2020, **4**, 243–256.
85 L. Zheng, Y. J. Wu, K. K. Li, G. Wang, C. Ma, C. S. Chen, P. Han, Y. Zhu, Z. H. Ke and Y. Chen, *ACS Mater. Lett.*, 2024, **6**, 4149–4157.
86 J. J. Ge, P. Q. Yin, Y. Chen, H. F. Cheng, J. W. Liu, B. Chen, C. L. Tan, P. F. Yin, H. X. Zheng, Q. Q. Li, S. M. Chen, W. J. Xu, X. Q. Wang, G. Wu, R. B. Sun, X. H. Shan, X. Hong and H. Zhang, *Adv. Mater.*, 2021, **33**, 2006711.
87 G. Wu, X. S. Zheng, P. X. Cui, H. Y. Jiang, X. Q. Wang, Y. T. Qu, W. X. Chen, Y. Lin, H. Li, X. Han, Y. M. Hu, P. G. Liu, Q. H. Zhang, J. J. Ge, Y. C. Yao, R. B. Sun, Y. Wu, L. Gu, X. Hong and Y. D. Li, *Nat. Commun.*, 2019, **10**, 4855.
88 Y. J. Tang, Y. Wu, W. Q. Xu, L. Jiao, Y. F. Chen, M. Sha, H. R. Ye, W. L. Gu and C. Z. Zhu, *Anal. Chem.*, 2022, **94**, 1022–1028.
89 N. L. Yang, H. F. Cheng, X. Z. Liu, Q. B. Yun, Y. Chen, B. Li, B. Chen, Z. C. Zhang, X. P. Chen, Q. P. Lu, J. T. Huang, Y. Huang, Y. Zong, Y. H. Yang, L. Gu and H. Zhang, *Adv. Mater.*, 2018, **30**, 1803234.
90 Y. Y. Ge, J. J. Ge, B. Huang, X. X. Wang, G. G. Liu, X. H. Shan, L. Ma, B. Chen, G. H. Liu, S. M. Du, A. Zhang, H. F. Cheng, Q. Wa, S. Y. Lu, L. J. Li, Q. B. Yun, K. Yuan, Q. X. Luo, Z. J. Xu, Y. H. Du and H. Zhang, *Nano Res.*, 2023, **16**, 4650–4655.
91 Z. Lyu, J. L. Cai, X. G. Zhang, H. Q. Li, H. P. Huang, S. P. Wang, T. Y. Li, Q. X. Wang, Z. X. Xie and S. F. Xie, *Adv. Mater.*, 2024, **36**, 2314252.
92 W. C. Wang, X. T. Shi, T. N. He, Z. R. Zhang, X. L. Yang, Y. J. Guo, B. Chong, W. M. Zhang and M. S. Jin, *Nano Lett.*, 2022, **22**, 70287033.
93 P. F. Yin, M. Zhou, J. Z. Chen, C. L. Tan, G. G. Liu, Q. L. Ma, Q. B. Yun, X. Zhang, H. F. Cheng, Q. P. Lu, B. Chen, Y. Chen, Z. C. Zhang, J. T. Huang, D. Y. Hu, J. Wang, Q. Liu, Z. Y. Luo, Z. Q. Liu, Y. Y. Ge, X. J. Wu, X. W. Du and H. Zhang, *Adv. Mater.*, 2020, **32**, 2000482.
94 W. C. Wang, T. O. He, X. L. Yang, Y. M. Liu, C. Q. Wang, J. Li, A. D. Xiao, K. Zhang, X. T. Shi and M. S. Jin, *Nano Lett.*, 2021, **21**, 3458–3464.
95 H. Y. Yan, Y. F. Chen, L. Jiao, W. L. Gu and C. Z. Zhu, *Sens. Actuators, B*, 2021, **341**, 130007.
96 X. F. Huang, G. X. Yang, S. Li, H. J. Wang, Y. H. Cao, F. Peng and H. Yu, *J. Energy Chem.*, 2022, **68**, 721–751.
97 X. W. Wei, G. X. Zhu, Y. J. Liu, Y. H. Ni, Y. Song and Z. Xu, *Chem. Mater.*, 2008, **20**, 6248–6253.
98 A. Amiri, V. Yurkiv, A. H. Phakatkar, T. Shokuhfar and R. Shahbazian-Yassar, *Adv. Funct. Mater.*, 2024, **34**, 2304685.
99 H. Y. Cheng, C. X. Wang, D. Qin and Y. A. Xia, *Acc. Chem. Res.*, 2023, **56**, 900–909.
100 R. Ferrando, J. Jellinek and R. L. Johnston, *Chem. Rev.*, 2008, **108**, 845–910.
101 S. S. Li, L. Shang, B. L. Xu, S. H. Wang, K. Gu, Q. Y. Wu, Y. Sun, Q. H. Zhang, H. L. Yang, F. R. Zhang, L. Gu, T. R. Zhang and H. Y. Liu, *Angew. Chem., Int. Ed.*, 2019, **58**, 12624–12631.
102 M. Zhou, C. Li and J. Y. Fang, *Chem. Rev.*, 2021, **121**, 736–795.
103 L. Kong, D. Chen, X. Zhang, L. Zhou, Y. Deng and S. Wei, *ACS Appl. Nano Mater.*, 2023, **6**, 3618–3626.
104 J. Liu, S. M. Dong, S. L. Gai, Y. S. Dong, B. Liu, Z. Y. Zhao, Y. Xie, L. L. Feng, P. P. Yang and J. Lin, *ACS Nano*, 2023, **17**, 20402–20423.
105 D. B. Yan, L. Jiao, C. J. Chen, X. K. Jia, R. M. Li, L. J. Hu, X. T. Li, Y. L. Zhai, P. E. Strizhak, Z. J. Zhu, J. G. Tang and X. Q. Lu, *Nano Lett.*, 2024, **24**, 2912–2920.
106 X. Zong, X. R. Xu, D. W. Pang, X. L. Huang and A. A. Liu, *Adv. Healthcare Mater.*, 2024, 2401836.
107 L. Zheng, L. Xu, P. Gu and Y. Chen, *Nanoscale*, 2024, **16**, 8672–8672.
108 S. Y. Xia, F. X. Wu, L. Cheng, H. B. Bao, W. P. Gao, J. Duan, W. X. Niu and G. B. Xu, *Small*, 2023, **19**, 2205997.
109 Y. L. Zhu, R. X. Zhao, L. Feng, C. Wang, S. M. Dong, M. V. Zyuzin, A. Timin, N. S. Hu, B. Liu and P. P. Yang, *ACS Nano*, 2023, **17**, 6833–6848.
110 B. Huang, Y. Y. Ge, A. Zhang, S. Q. Zhu, B. Chen, G. X. Li, Q. B. Yun, Z. Q. Huang, Z. Y. Shi, X. C. Zhou, L. J. Li, X. X. Wang, G. Wang, Z. Q. Guan, L. Zhai, Q. X. Luo, Z. J. Li, S. Y. Lu, Y. Chen, C. S. Lee, Y. Han, M. H. Shao and H. Zhang, *Adv. Mater.*, 2023, **35**, 2300490.
111 J. W. Liu, C. R. Lee, Y. Hu, Z. S. Liang, R. Ji, X. Y. D. Soo, Q. Zhu and Q. Y. Yan, *SmartMat*, 2023, **4**, e1210.
112 H. S. Chen, T. M. Benedetti, V. R. Goncales, N. M. Bedford, R. W. J. Scott, R. F. Webster, S. Cheong, J. J. Gooding and R. D. Tilley, *J. Am. Chem. Soc.*, 2020, **142**, 3231–3239.
113 S. M. Han, C. H. He, Q. B. Yun, M. Y. Li, W. Chen, W. B. Cao and Q. P. Lu, *Coord. Chem. Rev.*, 2021, **445**, 214085.
114 S. Furukawa and T. Komatsu, *ACS Catal.*, 2017, **7**, 735–765.
115 Y. L. Zhu, X. X. Wang, L. L. Feng, R. X. Zhao, C. Yu, Y. L. Liu, Y. Xie, B. Liu, Y. Zhou and P. P. Yang, *Nat. Commun.*, 2024, **15**, 8696.
116 C. H. Zhan, Y. Xu, L. Z. Bu, H. Z. Zhu, Y. G. Feng, T. Yang, Y. Zhang, Z. Q. Yang, B. L. Huang, Q. Shao and X. Q. Huang, *Nat. Commun.*, 2021, **12**, 6261.
117 F. X. Lin, M. G. Li, L. Y. Zeng, M. C. Luo and S. J. Guo, *Chem. Rev.*, 2023, **123**, 12507–12593.
118 J. T. Ren, L. Chen, H. Y. Wang and Z. Y. Yuan, *Chem. Soc. Rev.*, 2023, **52**, 8319–8373.
119 X. J. Chang, M. Q. Zeng, K. L. Liu and L. Fu, *Adv. Mater.*, 2020, **32**, 1907226.
120 Y. Q. Zhang, D. D. Wang and S. Y. Wang, *Small*, 2022, **18**, 2104339.
121 Y. J. Ai, M. Q. He, H. Sun, X. M. Jia, L. Wu, X. Y. Zhang, H. B. Sun and Q. L. Liang, *Adv. Mater.*, 2023, **35**, 2302335.
122 R. Sheng, Y. Liu, T. M. Cai, R. Wang, G. Yang, T. Wen, F. J. Ning and H. L. Peng, *Chem. Eng. J.*, 2024, **485**, 149913.
123 J. X. Feng, X. W. Yang, T. Du, L. Zhang, P. F. Zhang, J. C. Zhuo, L. P. Luo, H. Sun, Y. R. Han, L. Z. Liu,

Y. Z. Shen, J. L. Wang and W. T. Zhang, *Adv. Sci.*, 2023, **10**, 2303078.
124 M. Sha, L. Rao, W. Q. Xu, Y. Qin, R. A. Su, Y. Wu, Q. Fang, H. J. Wang, X. W. Cui, L. R. Zheng, W. L. Gu and C. Z. Zhu, *Nano Lett.*, 2023, **23**, 701–709.
125 Y. Y. Liang, F. Y. Sun, S. H. Qu, X. M. Zhou and L. Shang, *Sens. Actuators, B*, 2024, **417**, 136069.
126 Y. Chen, X. R. Yang, K. Li, J. K. Feng, X. Y. Liu, Y. X. Li, K. Y. Yang, J. H. Li and S. H. Ge, *ACS Nano*, 2024, **18**, 7024–7036.
127 K. Y. Wang, Q. Hong, C. X. Zhu, Y. Xu, W. Li, Y. Wang, W. H. Chen, X. Gu, X. H. Chen, Y. F. Fang, Y. F. Shen, S. Q. Liu and Y. J. Zhang, *Nat. Commun.*, 2024, **15**, 5705.
128 Y. H. Lin, Z. H. Li, Z. W. Chen, J. S. Ren and X. G. Qu, *Biomaterials*, 2013, **34**, 2600–2610.
129 J. S. Fan, X. Y. Zhang, W. L. Tan, Z. Z. Feng and K. Li, *Nano Lett.*, 2024, **24**, 7800–7808.
130 H. T. Shan, J. F. Shi, T. K. Chen, Y. T. Cao, Q. F. Yao, H. An, Z. C. Yang, Z. H. Wu, Z. Y. Jiang and J. P. Xie, *ACS Nano*, 2023, **17**, 23682377.
131 J. Zhou, X. J. Yang, Q. Yu, X. L. Li, H. Y. Chen and J. J. Xu, *ACS Appl. Nano Mater.*, 2022, **5**, 7009–7018.
132 H. Z. Fan, Y. Y. Li, J. B. Liu, R. Cai, X. S. Gao, H. Zhang, Y. L. Ji, G. J. Nie and X. C. Wu, *ACS Appl. Mater. Interfaces*, 2019, **11**, 45416–45426.
133 X. Liu, Y. L. Wan, T. Jiang, Y. F. Zhang, P. Huang and L. H. Tang, *Chem. Commun.*, 2020, **56**, 1784–1787.
134 Y. Kang, C. Li, H. L. Shi, A. Zhang, C. S. Huang, C. H. Zhou and N. Q. Jia, *Chin. J. Chem.*, 2023, **41**, 3189–3196.
135 C. Wang, Y. Shi, Y. Y. Dan, X. G. Nie, J. Li and X. H. Xia, *Chem. – Eur. J.*, 2017, **23**, 6717.
136 X. Q. Sang, S. Y. Xia, L. Cheng, F. X. Wu, Y. Tian, C. X. Guo, G. B. Xu, Y. L. Yuan and W. X. Niu, *Small*, 2024, **20**, 2305369.
137 J. K. Zhang, Y. Yang, F. M. Qin, T. T. Hu, X. S. Zhao, S. C. Zhao, Y. Q. Cao, Z. Gao, Z. Zhou, R. Z. Liang, C. L. Tan and Y. Qin, *Adv. Healthcare Mater.*, 2023, **12**, 2302056.
138 L. Zhao, Z. Q. Sun, Y. Wang, J. Huang, H. T. Wang, H. Li, F. Chang and Y. Y. Jiang, *Acta Biomater.*, 2023, **170**, 496–506.
139 M. S. Xu, R. X. Zhao, B. Liu, F. Geng, X. D. Wu, F. Zhang, R. F. Shen, H. M. Lin, L. L. Feng and P. P. Yang, *Chem. Eng. J.*, 2024, **491**, 151776.
140 X. R. Song, J. F. Liu, W. R. Wang, L. Ding, W. Feng, T. T. Zhang, Y. Chen and X. J. Ni, *Adv. Funct. Mater.*, 2024, **34**, 2312172.
141 Y. L. Zhu, Z. Wang, R. X. Zhao, Y. H. Zhou, L. L. Feng, S. L. Gai and P. P. Yang, *ACS Nano*, 2022, **16**, 3105–3118.
142 Y. Chen, J. B. Tan, Q. Zhang, T. Xin, Y. L. Yu, Y. Nie and S. Y. Zhang, *Nano Lett.*, 2020, **20**, 6548–6555.
143 X. L. He, L. F. Tan, D. Chen, X. L. Wu, X. L. Ren, Y. Q. Zhang, X. W. Meng and F. Q. Tang, *Chem. Commun.*, 2013, **49**, 4643–4645.
144 C. C. Wang, Y. Q. Li, W. J. Yang, L. Zhou and S. H. Wei, *Adv. Healthcare Mater.*, 2021, **10**, 2100601.
145 S. H. Ku, M. Lee and C. B. Park, *Adv. Healthcare Mater.*, 2013, **2**, 244–260.
146 Y. Sun, B. L. Xu, X. T. Pan, H. Y. Wang, Q. Y. Wu, S. S. Li, B. Y. Jiang and H. Y. Liu, *Coord. Chem. Rev.*, 2023, **475**, 214896.
147 H. Wang, K. W. Wan and X. H. Shi, *Adv. Mater.*, 2019, **31**, 1805368.
148 M. J. Liang, Y. B. Wang, K. Ma, S. S. Yu, Y. Y. Chen, Z. Deng, Y. Liu and F. Wang, *Small*, 2020, **16**, 2002348.
149 Y. J. Zhang, W. H. Gao, Y. A. Ma, L. L. Cheng, L. Zhang, Q. G. Liu, J. Y. Chen, Y. R. Zhao, K. S. Tu, M. Z. Zhang and C. Liu, *Nano Today*, 2023, **49**, 101768.
150 L. Fan, X. D. Xu, C. H. Zhu, J. Han, L. Z. Gao, J. Q. Xi and R. Guo, *ACS Appl. Mater. Interfaces*, 2018, **10**, 4502–4511.
151 L. Ma, F. B. Jiang, X. Fan, L. Y. Wang, C. He, M. Zhou, S. Li, H. R. Luo, C. Cheng and L. Qiu, *Adv. Mater.*, 2020, **32**, 2003065.
152 Y. R. Xu, Y. W. Ren, X. L. Liu, H. P. Li and Z. Y. Lu, *Acta Phys.-Chim. Sin.*, 2024, **40**, 2403032.
153 G. L. Kuang, Z. C. Wang, M. Bilal, Z. Y. Wang, Y. X. Feng, Y. J. Du and J. D. Cui, *Aggregate*, 2024, e724.
154 Y. Huang, M. T. Zhao, S. K. Han, Z. C. Lai, J. Yang, C. L. Tan, Q. L. Ma, Q. P. Lu, J. Z. Chen, X. Zhang, Z. C. Zhang, B. Li, B. Chen, Y. Zong and H. Zhang, *Adv. Mater.*, 2017, **29**, 1700102.
155 Y. F. Liu, Y. Cheng, H. Zhang, M. Zhou, Y. J. Yu, S. C. Lin, B. Jiang, X. Z. Zhao, L. Y. Miao, C. W. Wei, Q. Y. Liu, Y. W. Lin, Y. Du, C. J. Butch and H. Wei, *Sci. Adv.*, 2020, **6**, eabb2695.
156 Y. Liu, L. Y. Zhang, Q. G. Li, H. Dai, T. Xiang, G. Y. Yang and L. Li, *Anal. Chim. Acta*, 2021, **1146**, 24–32.
157 J. He, F. J. Xu, J. Hu, S. L. Wang, X. D. Hou and Z. Long, *Microchem. J.*, 2017, **135**, 91–99.
158 L. Zhang, S. L. Wang, G. H. Zhang, N. Shen, H. Chen, G. H. Tao, G. H. Tao, F. Yong, J. Fu, Q. H. Zhu and L. He, *Cell Rep. Phys. Sci.*, 2022, **3**, 101114.
159 Q. Q. Liu, C. C. Xu, S. Chu, S. Li, F. X. Wang, Y. M. Si, G. J. Mao, C. F. Wu and H. Wang, *J. Mater. Chem. B*, 2022, **10**, 10075–10082.
160 Y. Y. Yuan, X. X. Xi, T. Bao, P. G. Bian, F. Pei, X. H. Zhang, S. F. Wang and W. Wen, *J. Anal. Test.*, 2024, **8**, 278287.
161 Z. Sun, Q. S. Zhao, G. H. Zhang, Y. Li, G. L. Zhang, F. B. Zhang and X. B. Fan, *RSC Adv.*, 2015, **5**, 10352–10357.
162 Y. Q. Xu, J. B. Fei, G. L. Li, T. T. Yuan, X. Xu and J. B. Li, *Angew. Chem., Int. Ed.*, 2019, **58**, 5572–5576.
163 T. R. Lin, L. S. Zhong, J. Wang, L. Q. Guo, H. Y. Wu, Q. Q. Guo, F. F. Fu and G. N. Chen, *Biosens. Bioelectron.*, 2014, **59**, 89–93.
164 Z. Y. Ding, Z. Li, X. X. Zhao, Y. R. Miao, Z. F. Yuan, Y. Y. Jiang and Y. Z. Lu, *J. Colloid Interface Sci.*, 2023, **631**, 86–95.
165 N. Wu, Y. T. Wang, X. Y. Wang, F. N. Guo, H. Wen, T. Yang and J. H. Wang, *Anal. Chim. Acta*, 2019, **1091**, 69–75.
166 G. G. Yang, Y. Chen, R. Shi, R. R. Chen, S. S. Gao, X. Zhang, Y. Rao, Y. Lu, Y. C. Peng, Z. H. Qing and C. X. Song, *Molecules*, 2023, **28**, 3736.

167 S. R. Tang, M. L. Wang, G. W. Li, X. Li, W. Chen and L. Zhang, *Microchim. Acta*, 2018, **185**, 273.
168 C. Peng, R. Y. Pang, J. Li and E. R. Wang, *Adv. Mater.*, 2024, **36**, 2211724.
169 L. Jiao, H. Y. Yan, Y. Wu, W. L. Gu, C. Z. Zhu, D. Du and Y. H. Lin, *Angew. Chem., Int. Ed.*, 2020, **59**, 2565–2576.
170 L. Huang, J. X. Chen, L. F. Gan, J. Wang and S. J. Dong, *Sci. Adv.*, 2019, **5**, eaav5490.
171 S. F. Ji, B. Jiang, H. G. Hao, Y. J. Chen, J. C. Dong, Y. Mao, Z. D. Zhang, R. Gao, W. X. Chen, R. F. Zhang, Q. Liang, H. J. Li, S. H. Liu, Y. Wang, Q. H. Zhang, L. Gu, D. M. Duan, M. M. Liang, D. S. Wang, X. Y. Yan and Y. D. Li, *Nat. Catal.*, 2021, **4**, 407–417.
172 M. Y. Chang, Z. Y. Hou, M. Wang, C. Z. Yang, R. F. Wang, F. Li, D. L. Liu, T. L. Peng, C. X. Li and J. Lin, *Angew. Chem., Int. Ed.*, 2021, **60**, 12971–12979.
173 D. D. Wang, H. H. Wu, S. Z. F. Phua, G. B. Yang, W. Q. Lim, L. Gu, C. Qian, H. B. Wang, Z. Guo, H. Z. Chen and Y. L. Zhao, *Nat. Commun.*, 2020, **11**, 357.
174 R. J. Yan, S. Sun, J. Yang, W. Long, J. Y. Wang, X. Y. Mu, Q. F. Li, W. T. Hao, S. F. Zhang, H. L. Liu, Y. L. Gao, L. F. Ouyang, J. C. Chen, S. J. Liu, X. D. Zhang and D. Ming, *ACS Nano*, 2019, **13**, 11552–11560.
175 X. M. Shen, Z. Z. Wang, X. J. J. Gao and X. F. Gao, *Adv. Mater.*, 2024, **36**, 2211151.
176 W. W. He, Y. T. Zhou, W. G. Warner, X. N. Hu, X. C. Wu, Z. Zheng, M. D. Boudreau and J. J. Yin, *Biomaterials*, 2013, **34**, 765–773.
177 Y. Cheng, Y. D. Xia, Y. Q. Sun, Y. Wang and X. B. Yin, *Adv. Mater.*, 2024, **36**, 2308033.
178 J. N. Li, W. Q. Liu, X. C. Wu and X. F. Gao, *Biomaterials*, 2015, **48**, 37–44.
179 X. M. Shen, Z. Z. Wang, X. F. Gao and Y. L. Zhao, *ACS Catal.*, 2020, **10**, 12657–12665.
180 Y. Chong, Q. Liu and C. C. Ge, *Nano Today*, 2021, **37**, 101076.
181 S. B. He, L. Yang, X. L. Lin, L. M. Chen, H. P. Peng, H. H. Deng, X. H. Xia and W. Chen, *Talanta*, 2020, **211**, 120707.
182 P. Cheng, H. Wang and X. H. Shi, *Nanoscale*, 2020, **12**, 3050–3057.
183 R. Long, K. K. Mao, X. D. Ye, W. S. Yan, Y. B. Huang, J. Y. Wang, Y. Fu, X. S. Wang, X. J. Wu, Y. Xie and Y. J. Xiong, *J. Am. Chem. Soc.*, 2013, **135**, 3200–3207.
184 W. Q. Jiang, Y. Y. Feng, C. Jiang, H. Li, Z. Wang, Y. Q. Xiao, W. Lan and Y. N. Liu, *Sens. Actuators, B*, 2024, **412**, 135861.
185 M. Zhang, W. H. Yue, W. S. Ma, X. N. Wang, Y. H. Xu and A. H. Li, *Adv. Healthcare Mater.*, 2024, 2401602.
186 J. X. Chen, Q. Ma, M. H. Li, D. Y. Chao, L. Huang, W. W. Wu, Y. X. Fang and S. J. Dong, *Nat. Commun.*, 2021, **12**, 3375.
187 S. B. He, L. Yang, M. T. Lin, H. A. A. Noreldeen, R. X. Yu, H. P. Peng, H. H. Deng and W. Chen, *Sens. Actuators, B*, 2021, **347**, 130627.
188 A. Q. Lin, Z. Y. Sun, X. Q. Xu, S. Zhao, J. W. Li, H. Sun, Q. Wang, Q. Jiang, H. Wei and D. Q. Shi, *Nano Lett.*, 2022, **22**, 508–516.
189 J. Ming, T. B. Zhu, J. C. Li, Z. C. Ye, C. R. Shi, Z. D. Guo, J. J. Wang, X. L. Chen and N. F. Zheng, *Small*, 2021, **17**, 2103645.
190 M. Kajita, K. Hikosaka, M. Iitsuka, A. Kanayama, N. Toshima and Y. Miyamoto, *Free Radical Res.*, 2007, **41**, 615–626.
191 C. C. Ge, G. Fang, X. M. Shen, Y. Chong, W. G. Wamer, X. F. Gao, Z. F. Chai, C. Y. Chen and J. J. Yin, *ACS Nano*, 2016, **10**, 10436–10445.
192 H. Z. Fan, R. F. Zhang, K. L. Fan, L. Z. Gao and X. Y. Yan, *ACS Nano*, 2024, **18**, 2533–2540.
193 J. Y. Sheng, Y. H. Wu, H. Ding, K. Z. Feng, Y. Shen, Y. Zhang and N. Gu, *Adv. Mater.*, 2024, **36**, 2211210.
194 T. T. Cai, G. Fang, X. Tian, J. J. Yin, C. Y. Chen and C. C. Ge, *ACS Nano*, 2019, **13**, 12694–12702.
195 X. Y. Liu, X. Y. Liang, J. Yu, K. Y. Xu, J. W. Shen, W. Duan and J. B. Zeng, *TrAC, Trends Anal. Chem.*, 2023, **169**, 117386.
196 F. Arshad, N. F. Mohd-Naim, R. Chandrawati, D. Cozzolino and M. U. n. Ahmed, *RSC Adv.*, 2022, **12**, 26160–26175.
197 J. N. Xia, Z. Li, Y. P. Ding, L. A. Shah, H. B. Zhao, D. X. Ye and J. J. Zhang, *Anal. Chem.*, 2024, **96**, 8221–8233.
198 X. X. Zheng, Q. Liu, C. Jing, Y. Li, D. Li, W. J. Luo, Y. Q. Wen, Y. He, Q. Huang, Y. T. Long and C. H. Fan, *Angew. Chem., Int. Ed.*, 2011, **50**, 11994–11998.
199 C. Y. Zhou, Q. Wang, H. L. Cao, J. Jiang and L. Z. Gao, *Adv. Mater.*, 2024, **36**, 2403362.
200 Y. Tao, E. G. Ju, J. S. Ren and X. G. Qu, *Adv. Mater.*, 2015, **27**, 1097–1104.
201 B. Xiong, R. L. Xu, R. Zhou, Y. He and E. S. Yeung, *Talanta*, 2014, **120**, 262–267.
202 X. Y. Mu, J. Y. Wang, Y. H. Li, F. J. Xu, W. Long, L. F. Ouyang, H. L. Liu, Y. Q. Jing, J. Y. Wang, H. T. Dai, Q. Liu, Y. M. Sun, C. L. Liu and X. D. Zhang, *ACS Nano*, 2019, **13**, 1870–1884.
203 X. Li, X. Y. Ren, M. D. Xie, M. L. Zhu, Y. B. Zhang, T. Li, M. F. Huo and Q. Li, *Adv. NanoBiomed. Res.*, 2023, **3**, 2200144.
204 D. J. Wang, J. Wang, X. J. Gao, H. Ding, M. Yang, Z. H. He, J. Y. Xie, Z. X. Zhang, H. B. Huang, G. H. Nie, X. Y. Yan and K. L. Fan, *Adv. Mater.*, 2024, **36**, 2310033.
205 C. H. Wang, H. Y. Wang, B. L. Xu and H. Y. Liu, *VIEW*, 2021, **2**, 20200045.
206 S. Kang, Y. G. Gil, D. H. Min and H. Jang, *ACS Nano*, 2020, **14**, 4383–4394.
207 N. Tao, H. H. Li, L. Deng, S. F. Zhao, J. Ouyang, M. Wen, W. S. Chen, K. Zeng, C. W. Wei and Y. N. Liu, *ACS Nano*, 2022, **16**, 485–501.
208 M. Wang, M. Y. Chang, P. Zheng, Q. Q. Sun, G. Q. Wang, J. Lin and C. X. Li, *Adv. Sci.*, 2022, **9**, 2202332.